Using porphyry ore mineralization, in combination with geochemical and geological data to understand complex tectonomagmatic origins of magmatic belts: A regional study of the Absaroka, Challis, and Lowland Creek volcanic provinces of Idaho, Montana, and Wyoming, USA

by

Kyle C. Broley

B.S., University of Missouri – Kansas City, 2022

A THESIS

submitted in partial fulfillment of the requirements for the degree

MASTER OF SCIENCE

Department of Geology
College of Arts and Sciences

KANSAS STATE UNIVERSITY
Manhattan, Kansas

2024

Approved by:

Major Professor
Matthew Brueseke

Abstract

A significant part of the North American Cordillera contains a discontinuous north-northwestern trending chain of Eocene volcanic centers (e.g., the Challis-Kamloops volcanic belt), intermittently spanning > 2000 km from southern Idaho and Wyoming in the northwestern United States to central British Columbia in western Canada. The core area of this study is southern end of the Challis-Kamloops volcanic belt, specifically the Absaroka, central Idaho Challis, and Lowland Creek volcanic provinces of the central North American Cordillera. This study shows that a combination of regional differences in porphyry mineral systems (e.g., Cu- vs. Mo-dominated), combined with volcanic types and bulk rock geochemistry of igneous rocks, can be used to help decipher complex tectonomagmatic origins. Comparative Sr/Y versus wt% SiO_2 and (Eu/Eu*)/Yb data (e.g., mean Sr/Y = 77.1), coupled with Cu-porphyry deposits associated with an 230-km-long belt of stratovolcanoes, supports an arc origin for the Absaroka volcanic province. The central Idaho Challis volcanic province has chemical indices not conducive to Cu-porphyry mineralization (e.g., mean Sr/Y = 24.0), which, coupled with the presence of Mo-porphyry mineralization and a lack of stratovolcanoes, supports an extensional tectonomagmatic origin. Together, the disparate types of porphyry ore deposits, geochemical, and geologic data is used to create a new regional tectonic model to for the origins of the Absaroka, central Idaho Challis, and Lowland Creek volcanic provinces that involves the uneven subduction, tearing, and eventual foundering of the Farallon plate between 55 – 45 Ma.

Table of Contents

List of Figures

Acknowledgements

First, I would like to thank Dr. Matthew Brueseke for his support and guidance throughout my Graduate School journey. This thesis would not have been possible without you. Next, I would like to thank the members of my Thesis Committee, Dr. Pamela Kempton and Dr. Karin Goldberg. Their guidance and direction were invaluable in getting to this point. Finally, I thank my friends and family who supported me on this journey to continue my education. I would not have gotten here without them.

Chapter 1 - Introduction

A major part of the North American Cordillera contains a discontinuous north-northwestern trending chain of Eocene volcanic centers, intermittently spanning > 2000 km from southern Idaho and Wyoming in the northwestern United states to central British Columbia in western Canada (Dostal & Jutras, 2021). This magmatic belt, termed the Challis-Kamloops volcanic belt, is composed of a series of distinct semi-isolated volcanic provinces (Dostal & Jutras, 2021). The core area of this thesis is the Absaroka, central Idaho Challis, and Lowland Creek volcanic provinces of the current northern Rocky Mountain region, in the western and southern end of the Challis-Kamloops volcanic belt (Figure 1.1).

Eastward subduction of the Farallon plate beneath North America led to arc magmatism along the Cordilleran margin, which was accompanied by inboard deformation, during the Mesozoic (Armstrong & Ward, 1991; Dickinson, 2004). By the Late Cretaceous to Early Eocene, an increased rate of shortening across the foreland of the Sevier-Laramide orogen is recorded by shortening in the thin-skinned, Sevier fold and thrust belt (Dickinson et al., 1988; DeCelles, 2004; Wells et al., 2012). By ~54 - 49 Ma, a transition from shortening to extensional collapse of the thrust belt was underway and marked the end of the Laramide Orogeny (Constenius, 2003; Wells et al., 2012; Thoresen et al., 2024). In the northern Rockies, specifically northwest Wyoming, Idaho, and southwest Montana (USA), this tectonic change was accompanied by Challis-Absaroka province magmatism (Figure 1.2), as well as the development of extensional basins, more of which are adjacent to and associated with the Challis volcanic province (Janecke & Snee, 1993; Janecke et al., 1997; Schwartz & Schwartz, 2013). Regional metamorphic core complexes also started to form during the incipient period of extension (Howlett et al., 2021; Schwartz et al., 2019).

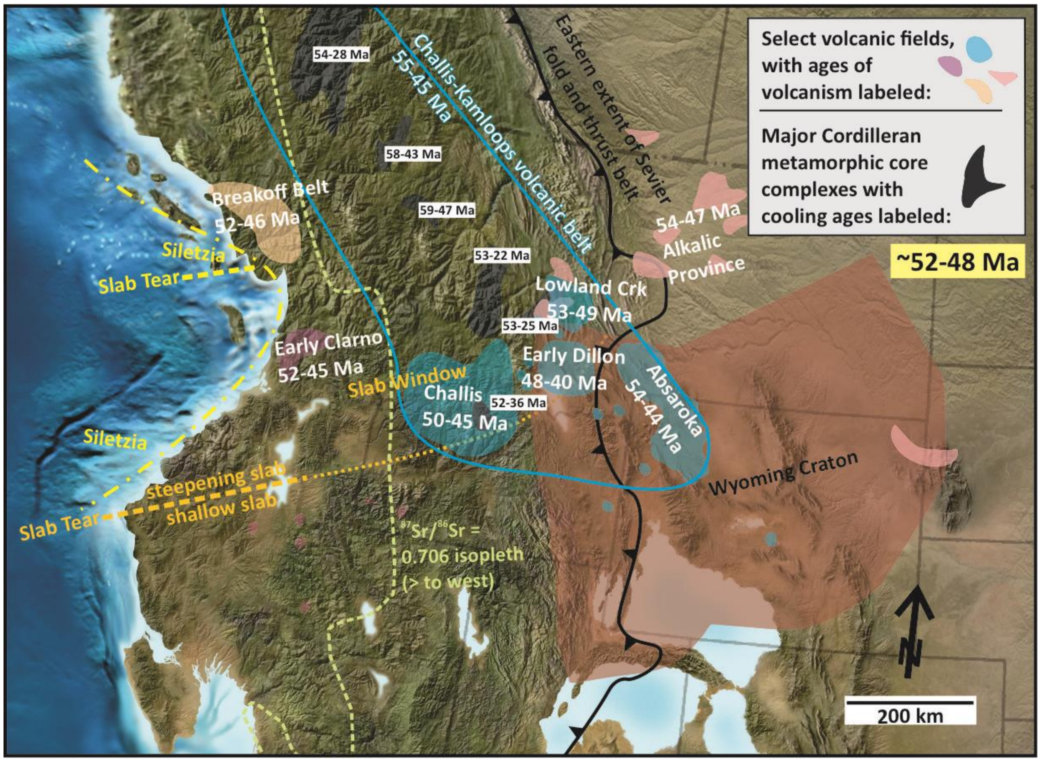

Figure 1.1 - Paleogeographic map of the northern Rockies and Pacific northwest (U.S.) and southern Canada at ~50 Ma. Also depicted are the Absaroka, Challis, and Lowland Creek volcanic provinces and ages when active (Norman & Mertzman, 1991;McKervey, 1998; Hiza, 1999; Feeley et al., 2002; Lindsay & Feeley, 2003; Dudás et al., 2010), early volcanism in the Dillon volcanic field (Fritz et al., 2007); Siletzia collision induced "Breakoff-belt" magmatism (Tepper et al., 2023), Challis-Kamloops volcanic belt(Dostal and Jutras, 2001), Montana/Great Plains alkalic province (Dudás and Harlan, 1999; Duke, 2009), early Clarno volcanism(Appel, 2002; Bestland et al., 2002), Wyoming craton extent (Bedrosian and Frost, 2023), Cordilleran core complexes and their cooling ages (Howlett et al., 2021),the inferred extent of Siletzia (Schmandt and Humphreys,2011), northern slab tear in Siletzia (Anderson et al., 2024), and slab tear along southern margin of Siletzia, separating steep-dipping, from shallow-dipping slab segments (Humphreys, 2009). Basemap© 2013 Colorado Plateau Geosystems Inc.

Challis-Absaroka magmatism is often suggested to represent the first "stage" of the ignimbrite flareup that swept southward across the central Cordillera from ~50 to 18 Ma (e.g., south through Nevada) (Figure 1.1) (Lipman et al., 1972; Coney, 1978; Best et al., 2016). This assertion directly links the sweep of magmatism to the effects of the Siletzia Plateau accretion (ca. ~51 – 48 Ma), causing removal of the shallow subducting Farallon Plate and exposure of the thinned and hydrated lithosphere to the infilling asthenosphere, generating voluminous magmatism (Humphreys, 2009; Best et al., 2016; Eddy et al., 2017; Humphreys & Grunder, 2022; Tepper & Clark, 2024). As the shallow slab was steepening and breaking off, it was apparently torn along a slab tear that extended northwestward, separated by a steeply dipping slab segment to the north, from a shallower-dipping segment to the south (Figure 1.1) (Humphreys, 2009; Colgan et al., 2011; Sigloch, 2011; Camp et al., 2017). The northern region, overlain by most of the Challis-Kamloops volcanic belt, was essentially over a slab window, or slab-free region (Figure 1.1) (Breitsprecher et al., 2003; Tepper & Clark, 2024). Siletzia accretion and this induced Farallon slab breakoff also led to establishment of the Cascades arc, ca. ~46 Ma, though that has been recently called into question by Tepper and Clark (2024).

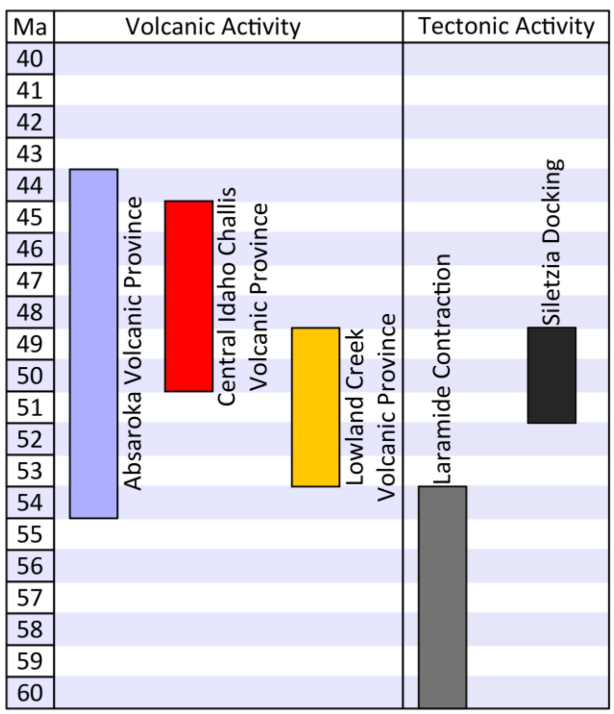

Figure 1.2 - Graph showing the timeline of regional volcanism, including the division of the Washburn, Sunlight, and Thorofare Creek groups of the Absaroka volcanic province (Norman & Mertzman, 1991; McKervey, 1998; Hiza, 1999; Feeley et al., 2002; Lindsay & Feeley, 2003; Dudás et al., 2010; Gaschnig et al., 2011; Scarberry, 2019) and significant regional tectonic events ((Humphreys, 2009; Best et al., 2016; Eddy et al., 2017; Humphreys & Grunder, 2022; Tepper & Clark, 2024 Thoresen et al., 2024).

The 54 – 44 Ma Absaroka volcanic province (Figure 1.2) consists of a northwest-trending series of stratovolcanoes, shield volcanoes, and dike swarms located mainly in northwestern Wyoming and extending into southern Montana (Sundell, 1993; Lindsay & Feeley, 2003; Feeley, 2003). The ~50 – 45 Ma central Idaho Challis volcanic province (Figure 1.2) were sourced from mafic and intermediate fissure vents and intermediate to felsic calderas in central and southwestern Idaho and is the largest Eocene volcanic province in comparison to other regional Eocene volcanics (Norman & Mertzman, 1991; Sanford, 2005; Dostal & Jutras, 2021). The ~52.9 – 48.6 Ma Lowland Creek volcanic province, is subordinate in volume to Challis and Absaroka provinces, but generally is temporally coincident and consists of an elongated northeast-southwest trending volcanic field made up of at least one caldera complex with resurgent domes in western Montana (Figure 1.2) (Dudás et al., 2010).

An often-overlooked component of regional Eocene magmatism in the central Cordillera, and the Challis and Absaroka provinces, are coeval, and temporarily coincident, porphyry mineral systems. Many porphyry ore systems originate from magmatically dominated hydrothermal fluids and most known Cu-porphyry deposits are genetically related to intermediate to felsic (52 – 77 wt % SiO_2) calc-alkaline magmas (e.g., hypabyssal intrusions below arc volcanoes) in volcanic arcs above active subduction zones (Richards, 2009; Ridley, 2013). Although magmas with these characteristics most commonly form directly in response to inputs from the subduction zone, it is also possible to extract compositionally and isotopically similar magmas, and associated hydrothermal systems, from upper plate lithosphere that has been modified by prior subduction processes (Richards, 2009; Holwell et al., 2019). These systems are inferred to be in response to a variety of mechanisms such as lithospheric thickening and thermal rebound, subcontinental lithospheric mantle (SCLM) delamination, or lithospheric extension (Richards, 2009). In contrast to Cu-rich porphyry systems that characterize volcanic arcs, porphyry systems can also be dominated by Mo-rich mineral systems (Taylor et al., 2012). Porphyry systems in extensional settings are usually less Cu-rich and dominated by Mo and W, and associated with high-Si rhyolite magmas, often sourced from calderas (Seedorff et al., 2005; Taylor et al., 2012). Thus, porphyry mineralization styles, combined with magma types and the physical volcanology of volcanoes for a given volcanic province, have the potential to clarify the tectono-magmatic origins of enigmatic belts of magmatism.

The geodynamic context for Eocene magmatism in the central Cordillera, including the Challis-Kamloops belt, is still debated (Glazner, 2022). Proposed tectonic models include the subduction of the Farallon plate (shallow or steeply dipping), coupled with post ~50 Ma rollback (Coney & Reynolds, 1977; Feeley et al., 2002; Dostal et al., 2003; Lindsay & Feeley, 2003; Li et al., 2021; Tikoff et al., 2023) or regional extension resulting from the post-Laramide orogenic plateau collapse (Norman & Mertzman, 1991; Gaschnig et al., 2011; Dostal & Jutras, 2021).

The goal of this study is to show that a combination of regional differences in porphyry mineral systems (e.g., Cu- vs. Mo-dominated) can be used, in combination with volcanic types and bulk rock geochemistry of igneous rocks, to decipher complex tectonomagmatic origins. This will be applied to the Eocene Absaroka, central Idaho Challis, and Lowland Creek volcanic provinces in the central region of the North American Cordillera to decipher their controversially complex tectono-magmatic origin.

Chapter 2 - Background of Regional Volcanic Provinces

2.1 Introduction

The key volcanic provinces of this study include the Absaroka volcanic province predominantly in Wyoming, the central Idaho Challis volcanic province, and the Lowland Creek volcanic province of western Montana. The selection of volcanic provinces is based on the availability of literature, geochemical data, age, and proximity to each other at the southern end of the Challis-Kamloops belt. Additionally, notable Eocene volcanic units exist throughout this region of the North American Cordillera, including the Dillon volcanics of Montana. However, this study does not include these units due to insufficient available or existing geochemical and isotope data. This chapter provides a general overview, geologic background, and geochemical analysis of the Absaroka, central Idaho Challis, and Lowland Creek volcanic provinces.

2.2 Absaroka Volcanic Province

The Absaroka volcanic province consists of a northwest-trending belt of stratovolcanoes, shield volcanoes, dike swarms, lavas, pyroclastic deposits, and thick packages of volcaniclastic sedimentary strata located predominantly in northwestern Wyoming, extending into southern Montana and part of eastern Idaho (Figure 2.1) (Chadwick, 1970; Smedes & Prostka, 1972; Fritz, 1982; Sundell, 1993; Feeley, 2003; Lindsay & Feeley, 2003). The Absaroka volcanic province comprises ~30,000 km^3 of basaltic to rhyolitic rocks distributed over an area exceeding 23,000 km^2, occupying a shallow Laramide foreland basin that formed concurrently with surrounding basement uplifts (Sundell, 1993; Feeley, 2003; Lindsay & Feeley, 2003). Based on field relationships and stratigraphy of the Eocene volcaniclastic and igneous units, the Absaroka

Supergroup is divided into the 54 Ma northern Washburn group, the 49 Ma Sunlight group, and the 47 Ma southern Thorofare Creek group (Figure 2.1) (Smedes & Prostka, 1972; Sundell, 1993).

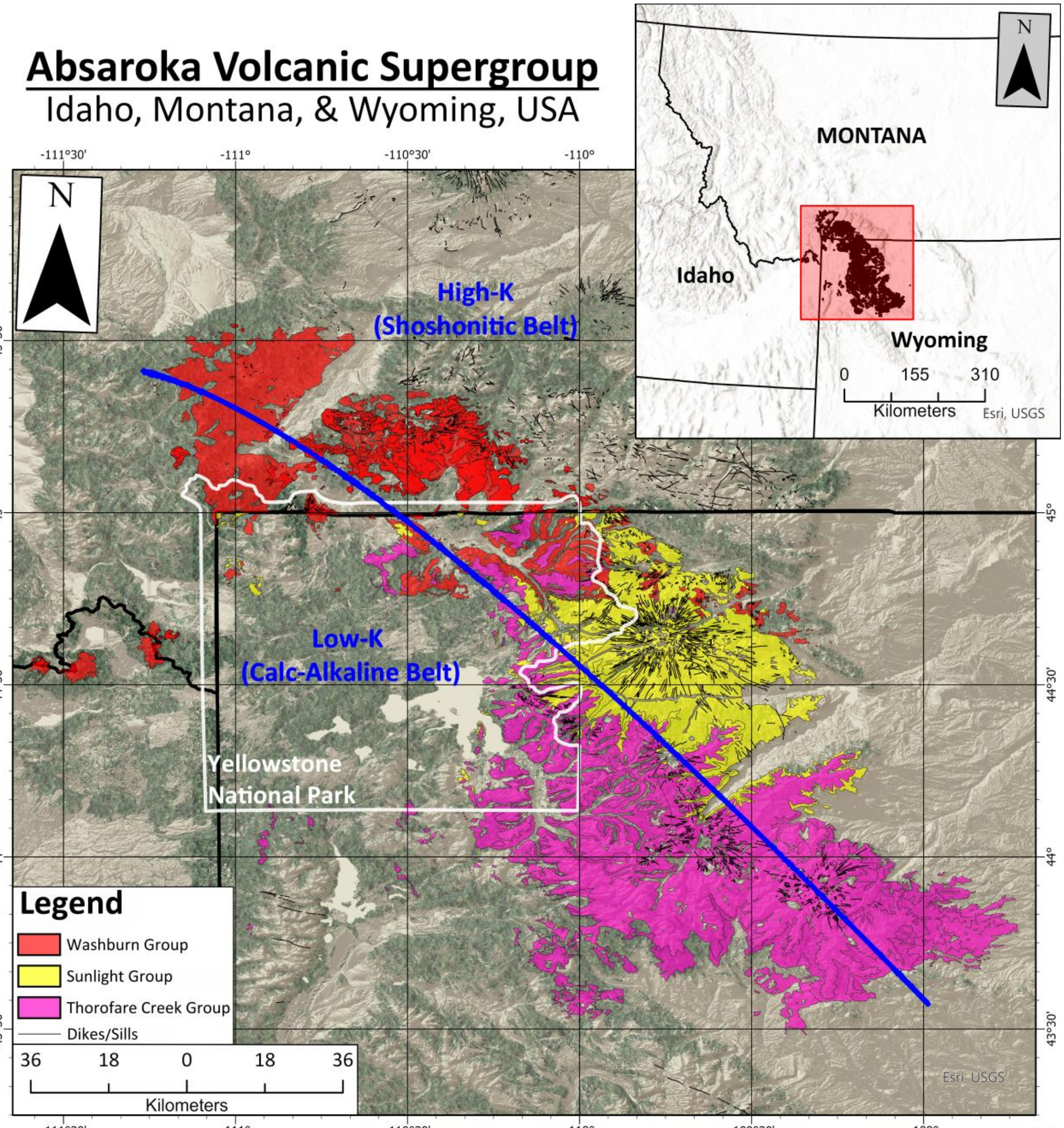

Figure 2.1 - Regional map of the Eocene Absaroka Volcanic Supergroup, separated by age of volcanism (53 Ma Washburn Group in red; 49 Ma Sunlight Group in yellow; 47 Ma Thorofare Creek Group in magenta), stratigraphy and geological unit mapping. Subset map is of the Absaroka Volcanic Province. Yellowstone National Park is highlighted in white for reference location. Dark bule line denotes the boundary between the eastern high-K shoshonitic belt and western low-K calc-alkaline belt (Vuke et al., 2013; Wyoming State Geological Survey, 2013; U.S. Geological Survey, 2013; U.S. Geological Survey, 2023).

$^{40}Ar/^{39}Ar$ dates from volcanic and intrusive rocks of the Absaroka volcanic province yield ages from 53 – 45 Ma, following or overlapping the latest phases of Laramide deformation (Hiza, 1999; Feeley et al., 2002; Feeley, 2003; Lindsay & Feeley, 2003). The Laramide orogenic belt, extending from New Mexico to Canada, is characterized by basement-cored uplifts and associated basins that formed during the Cretaceous and early Paleogene (Lageson et al., 2022). Uplift of the Archean basement accommodated horizontal crustal shortening across the Laramide foreland regionally (Lageson et al., 2022).

2.2.1 Geologic History

The Absaroka volcanic province rests unconformably on deformed Paleozoic to Mesozoic sedimentary strata and on the Wyoming Province's high-grade metamorphic and igneous crustal basement. This Archean craton underlies much of Wyoming, Montana, and southeastern Idaho (Figure 1.1) (Lindsay & Feeley, 2003; Bedrosian & Frost, 2023). Seismic refraction studies indicate that the continental crust beneath the Absaroka volcanic province is ~45 – 50-km-thick with the overall lithospheric thickness estimated to be at least 170-km-thick (Prodehl & Lipman, 1989; Iyer & Hitchcock, 1989; Feeley, 2003). The bulk of Absaroka volcanic province magmas erupted beginning with the 54 - 52 Ma Washburn group, followed by the 49 – 48 Ma Sunlight group, and ending with the 47 – 44 Ma Thorofare Creek group (Hiza, 1999; Feeley et al., 2002; Feeley, 2003; Lindsay & Feeley, 2003). The Absaroka volcanic province consists of 13 major volcanic centers situated along the subparallel western low-k (calc-alkaline) belt and eastern high – K (shoshonitic) belt (Figure 2.1) (Feeley, 2003). Although some of the Absaroka volcanic province is in Yellowstone National Park, it is much older and unrelated to the < 2.1 Ma Yellowstone Plateau volcanic field (Lindsay & Feeley, 2003). These nearly parallel belts likely reflect the occurrence of deep structural control (e.g., lithosphere-scale) on controlling magma ascent and thus stratovolcano occurrence (Chadwick, 1970; Feeley, 2003).

2.2.1.1 Wyoming Province

The Wyoming province is one of several large Archean cratonic blocks within the core of North America and located south of the Medicine Hat Block and Herne Province and west of the Superior Province (Figure 1.1) (Bedrosian & Frost, 2023). The Wyoming province, exposed in the cores of Laramide foreland uplifts, consists mainly of Neoarchean (2.8 – 2.6 Ga) granitoid intrusions, supra-crustal belts, and older gneiss (Yonkee & Weil, 2015). The lithosphere of the Wyoming province has a distinctive velocity structure that distinguishes it from adjacent younger lithosphere (Foster et al., 2006). Lithospheric thickness is estimated to be at least 170 km based on a weak low-velocity zone between 170 – 225 km depth (Prodehl & Lipman, 1989; Lindsay & Feeley, 2003).

2.2.1.2 Laramide Orogeny

The Laramide orogenic event in the western United States consisted of basement-involved uplifts with intervening basins and inboard migration of igneous activity from the continental margin magmatic arc in the western interior of the U.S. during the late Cretaceous-early Cenozoic (Dickinson, 2004; Yonkee & Weil 2015; Heller & Liu, 2016; Carrapa et al., 2019). Laramide-style (basement-involved) deformation formed east of the Sevier thrust front (Figure 1.1) in the western United States Cordillera (Jackson et al., 2019). During the late Cretaceous in southwestern Montana and northwestern Wyoming, the orogen consisted of an outboard accretionary belt, a continental-margin magmatic arc, and an eastward verging retroarc fold-thrust belt (Carrapa et al., 2019).

Regional Laramide deformation is broadly coincident with eastward shifting and local shutdown in arc magmatism, interpreted to record the developmental region of low-angle to shallow-slab subduction along the Cordilleran margin, with or without the involvement of a subducted oceanic plateau (e.g., conjugate Shatsky or conjugate Hess plateaux) (Liu et al., 2010; Weil & Yonkee, 2012; Copeland et al., 2017). Crustal weakening, resulting from lower-crustal hydration, has been invoked to explain the co-location of more extensive basement involved foreland shortening of the Laramide foreland (Erslev et al., 2022). Association of crustal hydration, caused by low-angle subduction, may have detached previously stable continental crust, and caused Laramide-style basement-involved detachment into the center of the North American continent (Erslev et al., 2022).

2.2.1.3 Post-Laramide Collapse and Extension (Eocene – Oligocene)

A transition from shortening to extension marked the end of the Laramide orogeny (Wells et al., 2012; Weeks, 2022). Shortening ended between 54 – 51 Ma and extensional collapse of the thrust belt began by 49 Ma (Wells et al., 2012). Eocene extension was driven by the combination of gravitational potential energy resulting from thickened Sevier-Laramide crust, removal of the Farallon slab, upwelling asthenosphere, and a decrease in compressional forces across the plate boundary (Constenius, 1996; Wells et al., 2012). Eocene extension affected a wide region, including southwestern Montana and adjacent Idaho (Constenius, 1996; Schwartz & Schwartz, 2013).

2.2.2 Geochemistry of the Absaroka Volcanic Province

The Absaroka volcanic province suite is composed mainly of rocks with a broad spectrum of mafic to intermediate compositions with well-defined calc-alkaline arrays (Figure 2.2A) (Hiza, 1999). Samples from the Washburn Group form a medium- to high-K calc-alkaline suite in composition from basaltic andesite through rhyolite (Feeley et al., 2002). Sunlight and Thorofare Creek Group lavas have a wider range of compositions than the Washburn Group, with dominant basaltic trachyandesitic and trachyandesitic rock types (Hiza, 1999). Washburn Group rocks are dominantly subalkaline (e.g., calc-alkaline) (Figure 2.2B).

Major element diagrams for the sample suite (Figure 2.3) show strong linear arrays for wt% FeO*, TiO_2, and CaO decreasing compared to an increase in wt% SiO_2 (Feeley et al., 2002). Additionally, the Washburn Group rocks have positive arrays for wt% Na_2O and K_2O compared to wt% SiO_2. The remaining major elements of the Washburn, Sunlight, and Thorofare Creek Group samples have more dispersed chemical data distributions (Feeley et al., 2002).

The Absaroka volcanic province samples suite (Figure 2.4) is broadly characterized by enrichment of large ion lithophile elements compared to primitive mantle (Lindsay & Feeley, 2003). The suite is also characterized by a relative depletion in high field strength elements compared to primitive mantle (Lindsay & Feeley, 2003). The Thorofare Creek Groups has the least amount of variation in trace element compositions compared to the Washburn and Sunlight Groups. The Washburn and Thorofare Creek Group have less depletion in high field strength elements compared to the Sunlight Group.

The Nd and Sr isotope ratios for the Washburn Group rocks have relationships of many other volcanic suites resulting from assimilation of or mixing with continental crust, suggesting that crustal material was important to their genesis (Feeley et al., 2002). Whole-rock Sr and Nd isotope data for the Sunlight Group suggests crustal contamination, crystallization differentiation, and crystal accumulation were important for their creation (Feeley & Cosca, 2003). The overall arrays in Sr and Nd isotopes for the Thorofare Creek Group rocks suggest that magma is sourced from progressively shallower sources, followed by a deeper mantle source (e.g., primarily lithospheric) (Hiza, 1999; Feeley, 2003).

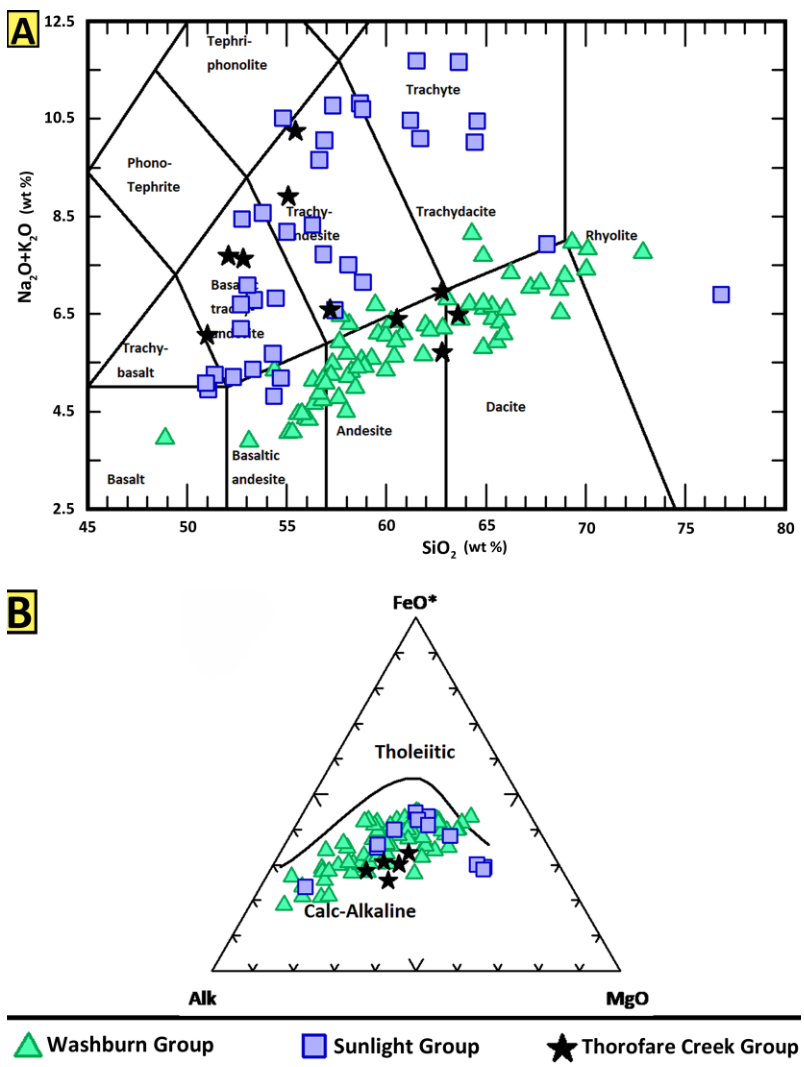

Figure 2.2 - (A) Total alkali versus silica diagram for the Absaroka volcanic province (Washburn Group shown by green triangles; Sunlight Group shown by blue squares; Thorofare Creek Group shown by black stars) with the Le Maitre et al., (1989) classification. (B) AFM diagram for the subalkaline series of the Absaroka volcanic province (Hiza, 1999; Feeley et al., 2002; Lindsay & Feeley, 2003).

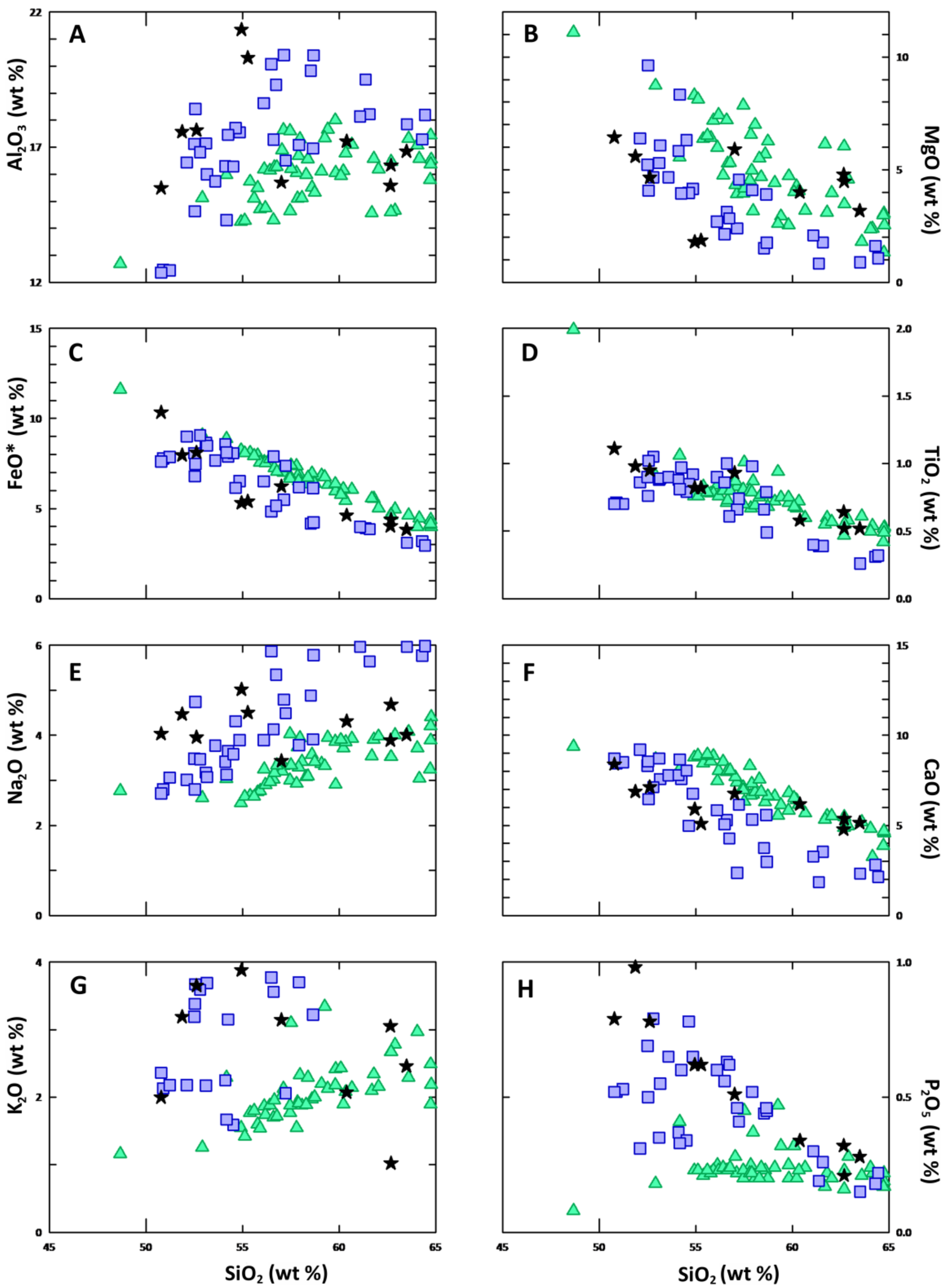

Figure 2.3 - Major element versus silica diagrams of the Washburn, Sunlight, and Thorofare Creek Groups of the Absaroka volcanic province (symbols same as in Figure 2.2) (Hiza, 1999; Feeley et al., 2002; Lindsay & Feeley, 2003).

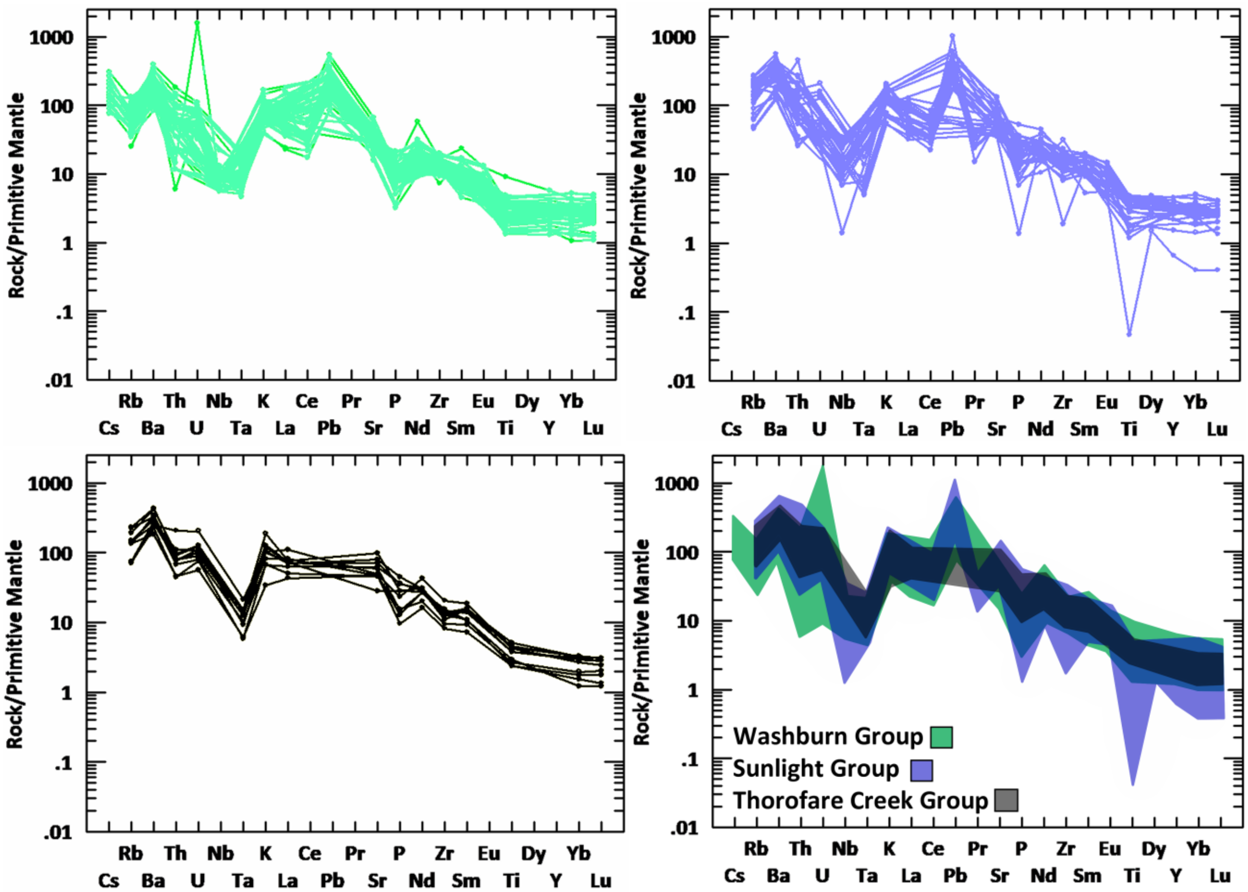

Figure 2.4 - Primitive mantle-normalized multi-element diagrams using the normalization of Sun and McDonough (1989) for the Absaroka volcanic province divided into the Washburn, Sunlight, and Thorofare Creek unit Groups and a comparative diagram of the entire sample suite (Hiza, 1999; Feeley et al., 2002; Lindsay & Feeley, 2003).

2.3 Central Idaho Challis Volcanic Province

The central Idaho Challis volcanic province, referred here as the Challis volcanic province, comprises mafic, intermediate, and silicic lavas and tuffs, as well as interbedded volcaniclastic deposits, that were sourced from fissure vents and calderas in central and southwestern Idaho between ~50 – 45 Ma (Figure 2.5) (Norman & Mertzman, 1991; Dostal & Jutras, 2021). The Challis volcanic province is the largest Eocene volcanic province in comparison to other regional volcanic provinces like the Absaroka and Lowland Creek volcanics (Sanford, 2005; Dostal & Jutras, 2021). Where well documented, Challis volcanic province pyroclastic deposits and lavas are up to 2.5 km-thick and overall, deposits cover > 25,000 km^2 area (Sanford, 2005; Dostal & Jutras, 2021). The eruptive history of the Challis volcanic province is divided into early effusive volcanism, followed by caldera-forming ash-flow tuff eruptions, and late-stage intrusions of domes and plugs (Sanford, 2005). Challis volcanic province rocks have high-K, calc-alkaline compositions and include minor shoshonites (Norman & Mertzman, 1991; McKervey, 1998; Dostal & Jutras, 2021).

Depositional relationships of the Challis volcanic province are complex due to a large topographic relief on the pre-Challis surface, the multitude of volcanic centers, and the relative inaccessibility of exposures (Sanford, 2005). The Challis volcanic province was deposited on an irregular pre-volcanic terrane consisting of Precambrian through Cretaceous batholiths and sedimentary strata with more than 300 m of structural and topographic relief (McKervey, 1998). Compression and peak metamorphism were associated with significant crustal thickening, suggesting that the Challis volcanic province erupted through continental crust that was ~40 – 45-km-thick (McKervey, 1998).

2.3.1 Geologic History

Challis magmatism in Idaho was a brief, voluminous magmatic event that resulted in thick accumulations of effusive and explosive volcanics (McKervey, 1998). The two general groups identified within the Challis volcanic province consist of a lower sequence of mafic to intermediate lavas and an upper sequence of more silicic ash-flow tuffs and lavas (Norman & Mertzman, 1991). The lower sequence of the Challis volcanic province overlies a basal conglomerate and is predominantly mafic-intermediate effusive lavas and breccias with minor pyroclastics derived from scattered vent and small down complexes (McKervey, 1998). The upper sequence is overlain by multiple explosive eruptions derived from large, nested caldera complexes (McKervey, 1998).

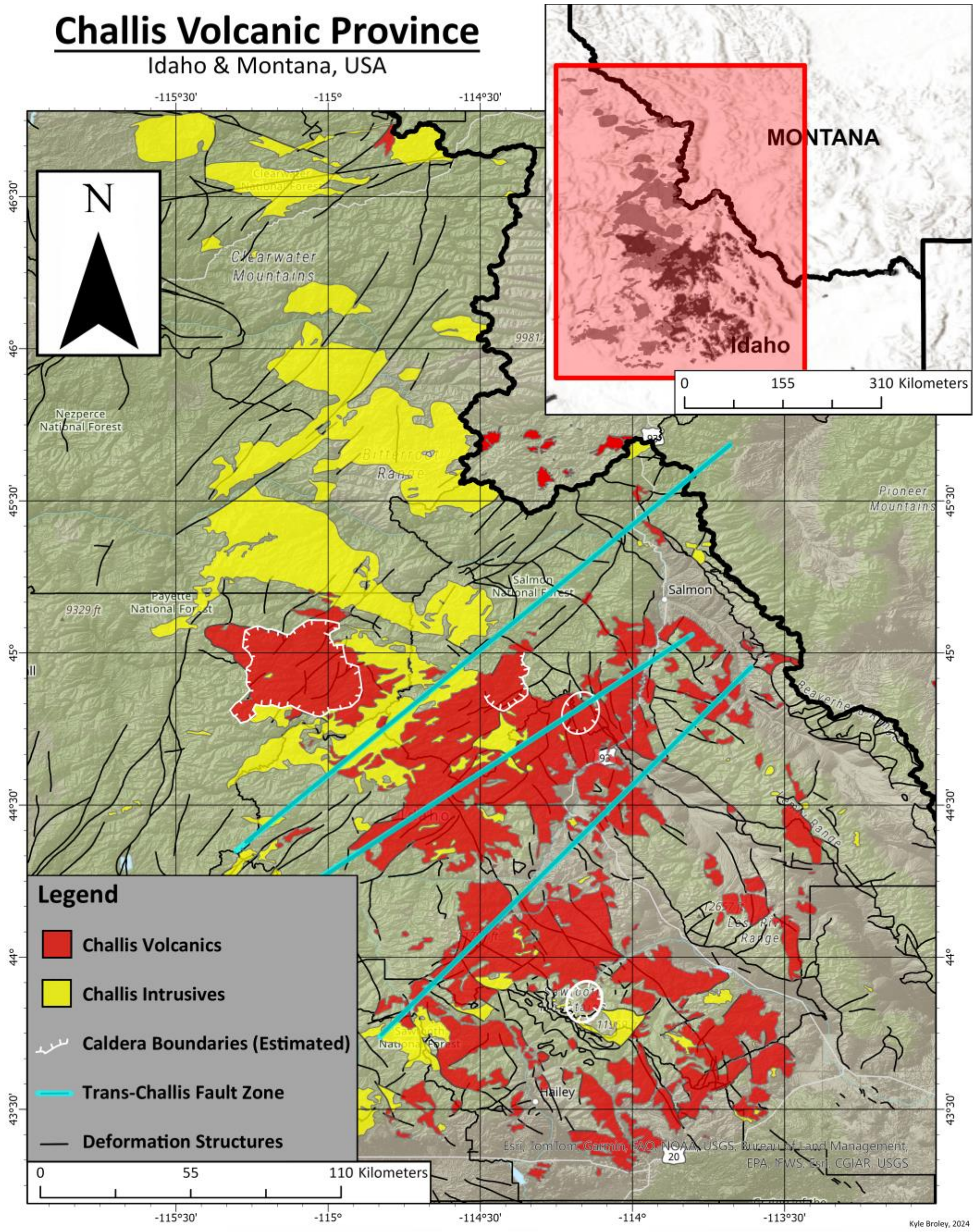

Figure 2.5 - Map of the Eocene central Idaho Challis volcanic province, divided into the Challis volcanics and Challis intrusives. Caldera structural boundaries are estimated, outlined in white. The Trans-Challis Fault System is shown in blue. Subset shows the regional location of the central Idaho Challis volcanic province, highlighted in red. Not depicted are Eocene rocks mapped as Challis volcanics south of the Snake River plain (e.g., Owyhee Mountains and vicinity, ID) (Lewis et al., 2012; Vuke et al., 2013; U.S. Geological Survey, 2019; U.S. Geological Survey, 2022; U.S. Geological Survey, 2023).

2.3.1.1 Idaho Batholith

The 98 – 53 Ma Idaho batholith is unique from other major North American Cordillera batholiths, because it is primarily characterized by peraluminous compositions and emplaced in Precambrian continental crust (Gaschnig et al., 2011). The other Cordilleran batholiths are characterized by primarily metaluminous compositions and found mostly within accreted juvenile crust (Gaschnig et al., 2011). All units of the Idaho batholith are cut by Eocene plutons and dikes, associated with the Challis volcanic province in east-central Idaho (Gaschnig et al., 2011). These intrusives are depicted on Figure 2.5.

2.3.1.2 Trans-Challis Fault System

A prominent regional structural feature known as the Trans-Challis Fault System appears to influence the nature of the Challis volcanic province magmatism (McKervey, 1998). The Trans-Challis Fault System is a northeast-trending zone up to 24-km-wide of numerous, closely spaced, Eocene normal faults (McKervey, 1998). Situated on this tectonic lineament are some of the major caldera structures of the Challis volcanic province, major grabens, numerous late-stage dike swarms, and significant porphyry mineralization (McKervey, 1998).

2.3.2 Geochemistry of the central Idaho Challis Volcanic Province

Challis volcanic province rocks are predominantly basaltic-trachyandesites, trachyandesites, and dacites (Figure 2.6A) (McKervey, 1998). Challis intrusives are dominantly dacite, trachydacite and trachyte, and rhyolite. The Challis sample suite plot as transitional subalkaline to mildly alkaline (McKervey, 1998). The Challis volcanic province rocks plot dominantly calc-alkaline (Figure 2.6B). With increasing wt% SiO_2 (Figure 2.7), the concentrations of TiO_2, FeO, MgO, CaO, and P_2O_5 in the Challis volcanic province samples tend to decrease. In the Challis volcanic units Al_2O_3, Na_2O, and K_2O increase, while the Challis intrusives decrease in Al_2O_3 with increasing wt% SiO_2 (Norman & Mertzman, 1991; McKervey, 1998; Gaschnig et al., 2011).

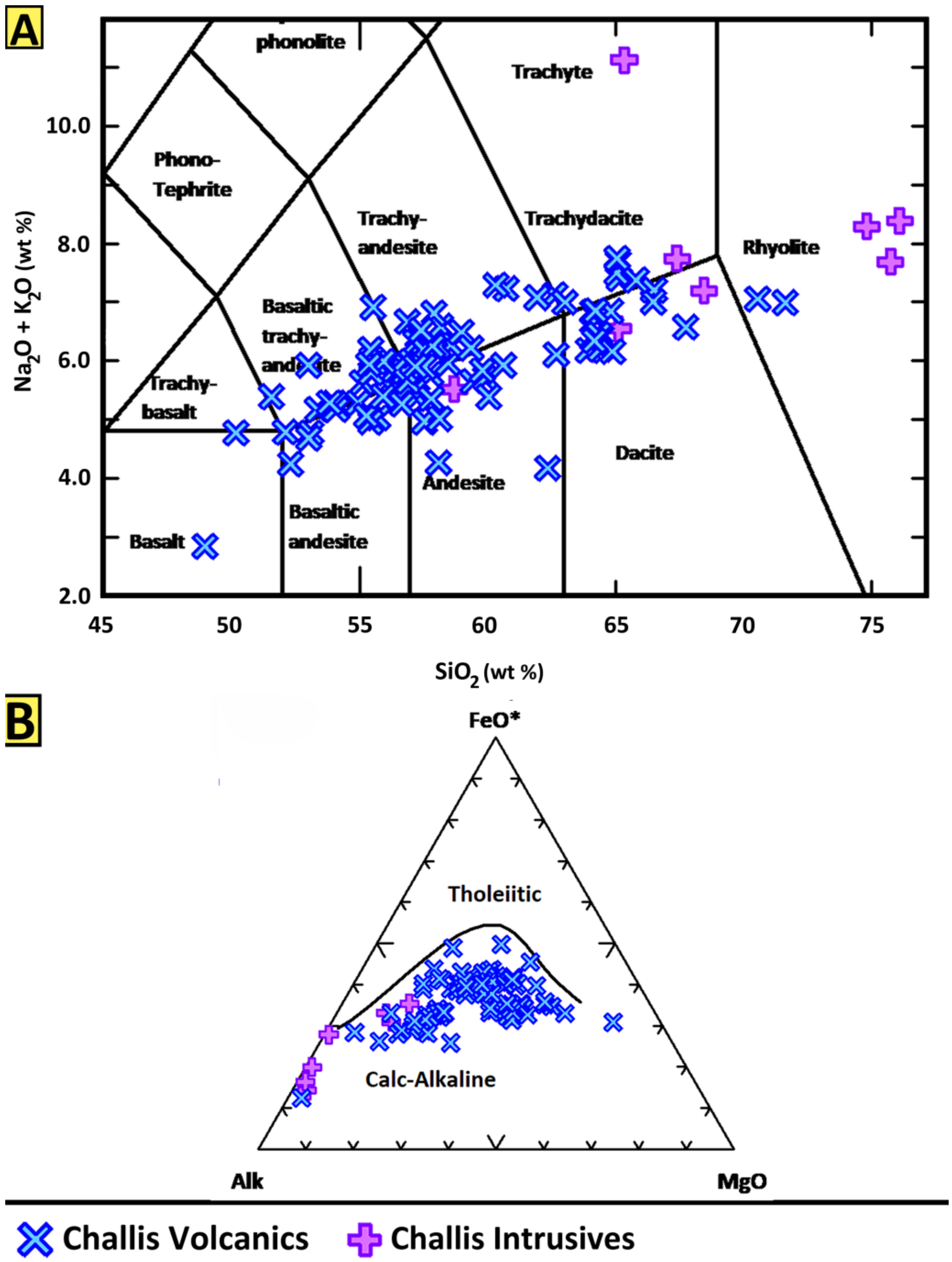

Figure 2.6 - Figure 2.6 - (A) Total alkali versus silica diagram for the Challis Volcanic Province with the classification of Le Maitre et al. (1989). (B) AFM diagram for the subalkaline series of the Challis volcanic province (volcanics from Norman & Mertzman, 1991; McKervey, 1998; intrusives from Gaschnig et al., 2011).

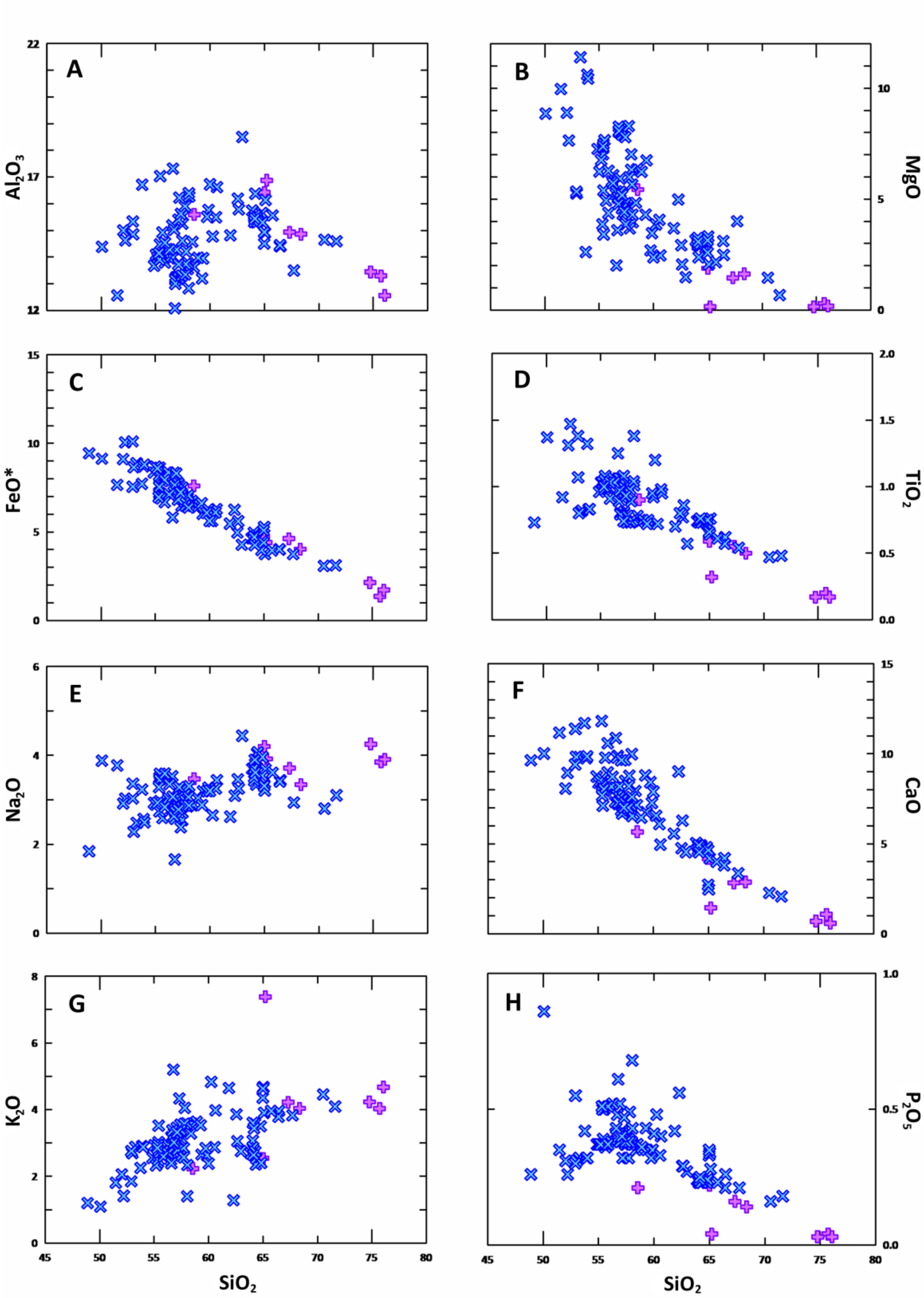

Figure 2.7 - Major element versus silica variation diagrams of the Challis volcanics and Challis intrusives of the Challis volcanic province (Norman & Mertzman, 1991; McKervey, 1998; Gaschnig et al., 2011).

The Challis volcanic province sample suite (Figure 2.8) is characterized by the enrichment of large ion lithophile elements and by a relative depletion in the high field strength elements relative to primitive mantle (Norman & Mertzman, 1991; McKervey, 1998; Gaschnig et al., 2011). Both units have similar patterns of rare earth element distributions compared to the Absaroka volcanic province. The Nd, Sr, and Pb isotopic ratios for the central Idaho Challis volcanic province rocks reflect partial melting of enriched lithospheric mantle and melts that variably interacted with continental crust (Norman & Mertzman, 1991; McKervey, 1998; Gaschnig et al., 2011). The Nd and Sr isotopic ratios for the effusive products of the central Idaho Challis volcanic province reinforce these interpretations (Norman & Mertzman, 1991; McKervey, 1998).

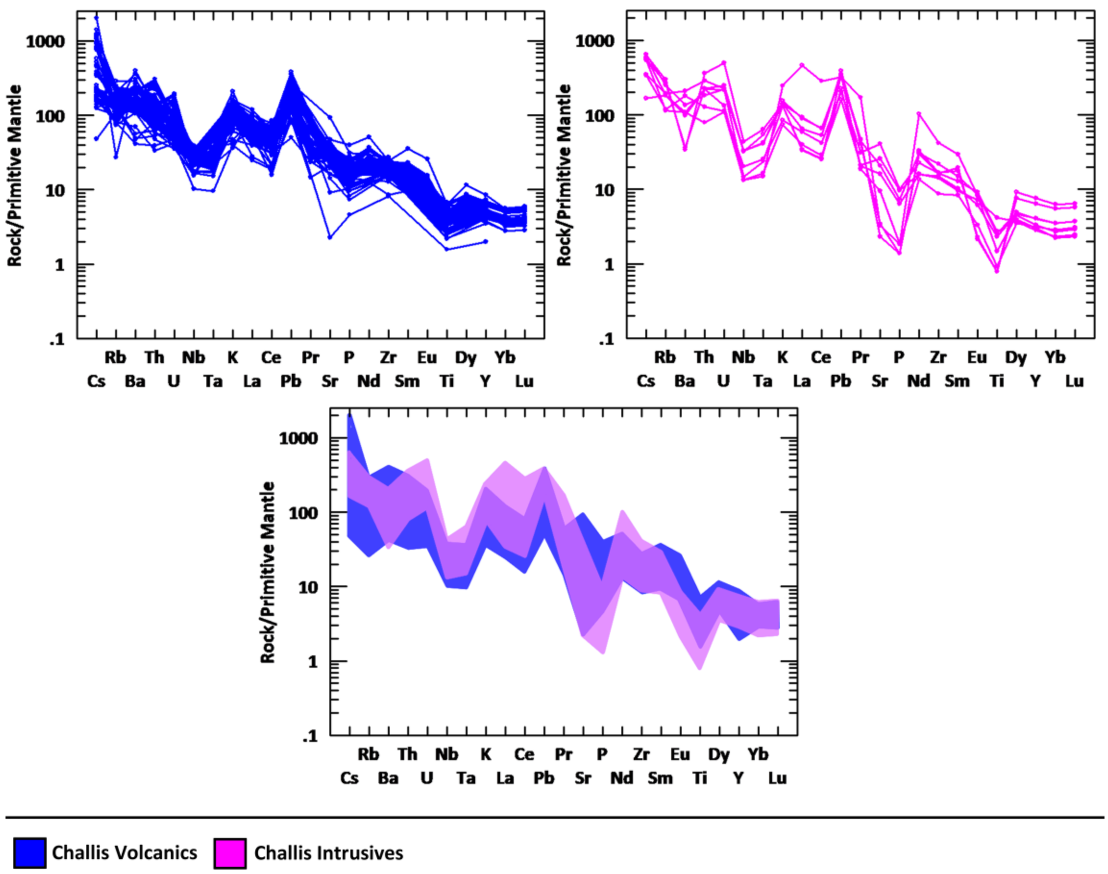

Figure 2.8 - Primitive mantle-normalized multi-element diagrams using the normalization of Sun and McDonough (1989) for the Challis volcanic province divided into the Challis volcanics, the Challis intrusives, and comparative diagrams (Norman & Mertzman, 1991; McKervey, 1998; Gaschnig et al., 2011).

2.4 Lowland Creek Volcanic Province

The Lowland Creek volcanic province (Figure 2.9) in western Montana is an elongated northeast-southwest trending volcanic field that fills a half-graben bounded on the southeast by an Eocene age normal fault that displaces the upper Cretaceous Boulder batholith (Dudás et al., 2010). The Lowland Creek volcanic province is divided into six laterally discontinuous units that form two cycles (Smedes, 1962; Dudás et al., 2010). The lower cycle consists primarily of tuffs, tuff breccias, and volcaniclastic sedimentary rocks, where the upper cycle consists dominantly of lavas (Dudás et al., 2010).

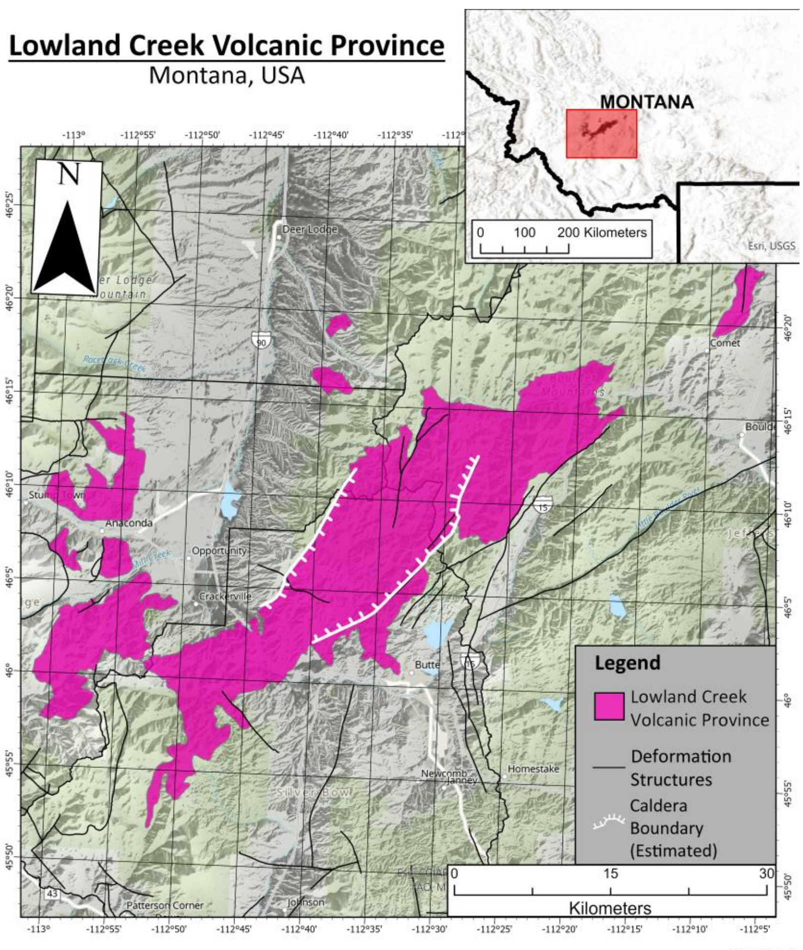

Figure 2.9 - Regional map of the Eocene Lowland Creek Volcanic Province showing local deformation structures and LCVP caldera boundary. Subset shows the regional location of the Lowland Creek Volcanic Province (Foster, 1987; Vuke et al., 2013; Geological Survey, 2013).

The $^{40}Ar/^{39}Ar$ dates of the Lowland Creek volcanic province show magmatism occurred from ~52.9 to 48.6 Ma, establishing that it was active contemporaneously with the calc-alkaline Absaroka and Challis magmatic events (Dudás et al., 2010). The volume and size of the Lowland Creek volcanic province require the participation of mantle melts as a heat source, though erupted products of this province only have a limited compositional range from andesite to rhyolite (Dudás et al., 2010; Young-Dahl, 2021).

2.4.1 Geologic History

The Lowland Creek volcanic province covers an estimated area of about 2000 km^2 and has an aggregate thickness of 2 km (Smedes, 1962; Dudás et al., 2010). The Lowland Creek volcanic province can be characterized by multiple large, tuff-forming eruptions characterized by caldera complexes with a resurgent dome complex northwest of Butte, Montana (Dudás et al., 2010). In most places, the Lowland Creek volcanic province directly overlies rocks of the upper Cretaceous Boulder batholith and the Elkhorn Mountain Volcanics (Dudás et al., 2010).

Boulder Batholith

The upper Cretaceous aged Boulder batholith encompasses about 4000 km^2 in southwest Montana (du Bray et al., 2012). The batholith lies in the Helena embayment of the Mesoproterozoic belt Supergroup and the foreland of the Late Cretaceous fold and thrust belt (du Bray et al., 2012). The Boulder batholith consists of a series of related plutons emplaced into Mesoproterozoic to Mesozoic sedimentary rocks and into cogenetic rocks of the Late Cretaceous Elkhorn Mountains Volcanics (du Bray et al., 2012).

2.4.2 Geochemistry of the Lowland Creek Volcanic Province

The whole rock compositions of the Lowland Creek volcanic province lavas and tuffs range from 60 – 76 wt% SiO_2 and range from andesite to rhyolite (Figure 2.10A) (Dudás et al., 2010). Moderately to strongly altered rhyolitic and rhyodacitic tuffs are volumetrically dominant with the Lowland Creek volcanic province, but dacite is the dominant lithology among the less altered lavas (Dudás et al., 2010). The major element compositions of the Lowland Creek volcanic province are subalkaline and calc-alkaline, with somewhat elevated alkali element contents in rocks above ~70 wt% SiO_2 (Figure 2.10B) (Dudás et al., 2010). With increasing wt% SiO_2 (Figure 2.11), Al_2O_3, MgO, FeO, TiO_2, Cao, and P_2O_5 concentrations in the Lowland Creek volcanic province sample suite show linear decreasing arrays (Dudás et al., 2010). K_2O has a more diffuse positive array with increased wt% SiO_2 content, while Na_2O has no identifiable array (Dudás et al., 2010). The Lowland Creek volcanic province sample suite (Figure 2.12) is characterized by the enrichment of LILEs and a relative depletion in the high-field strength elements, relative to primitive mantle (Dudás et al., 2010). The Nd and Pb isotopic compositions of the Lowland Creek volcanic province rocks suggest that the province is the product of mixing between the lithospheric mantle and lower and middle crust (Dudás et al., 2010).

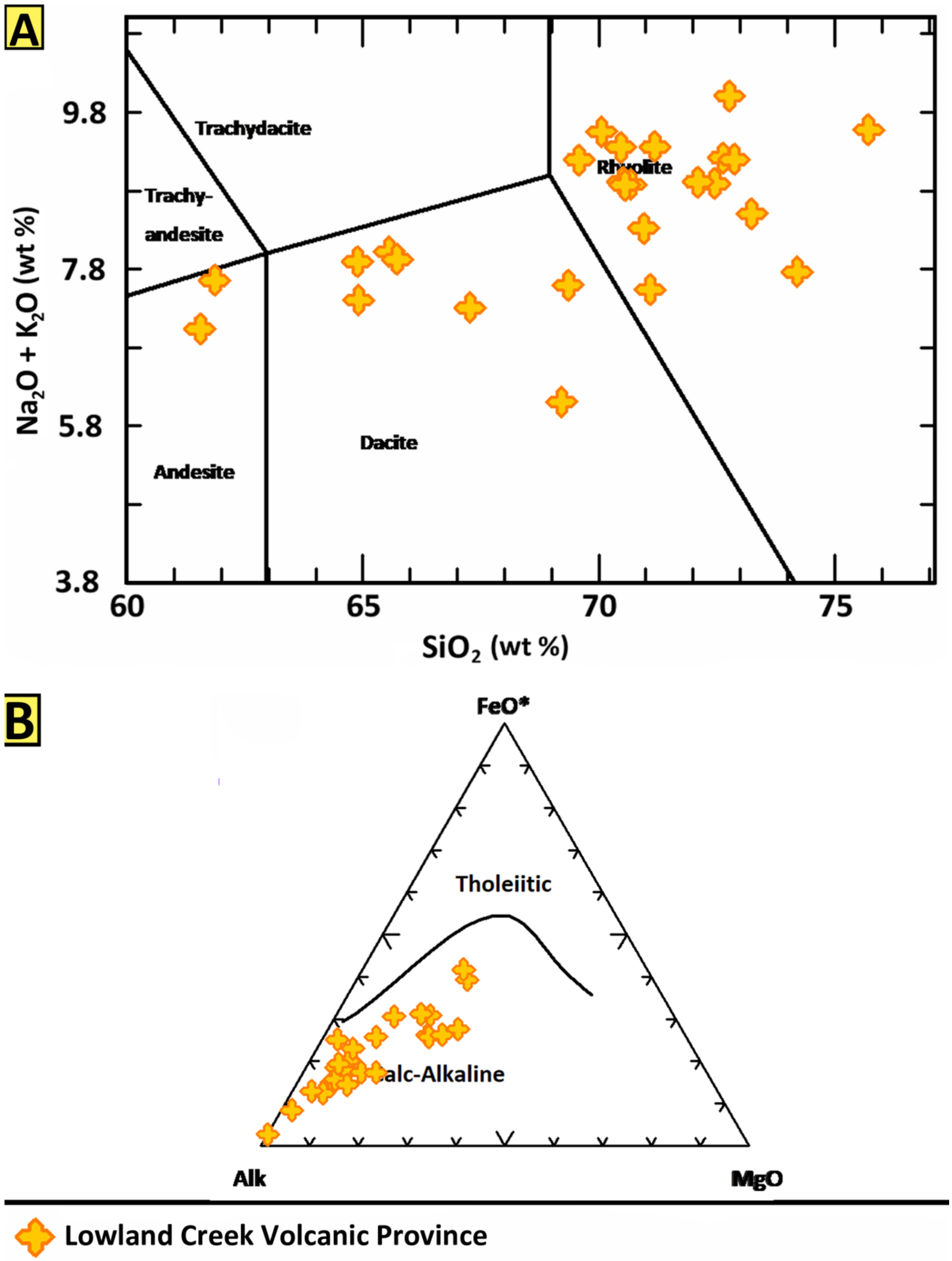

Figure 2.10 - (A) Total alkali versus silica diagram for the Lowland Creek volcanic province with the classification of Le Maitre et al. (1989). (B) AFM diagram for the Lowland Creek volcanic province (Dudás et al., 2010; Scarberry, 2019).

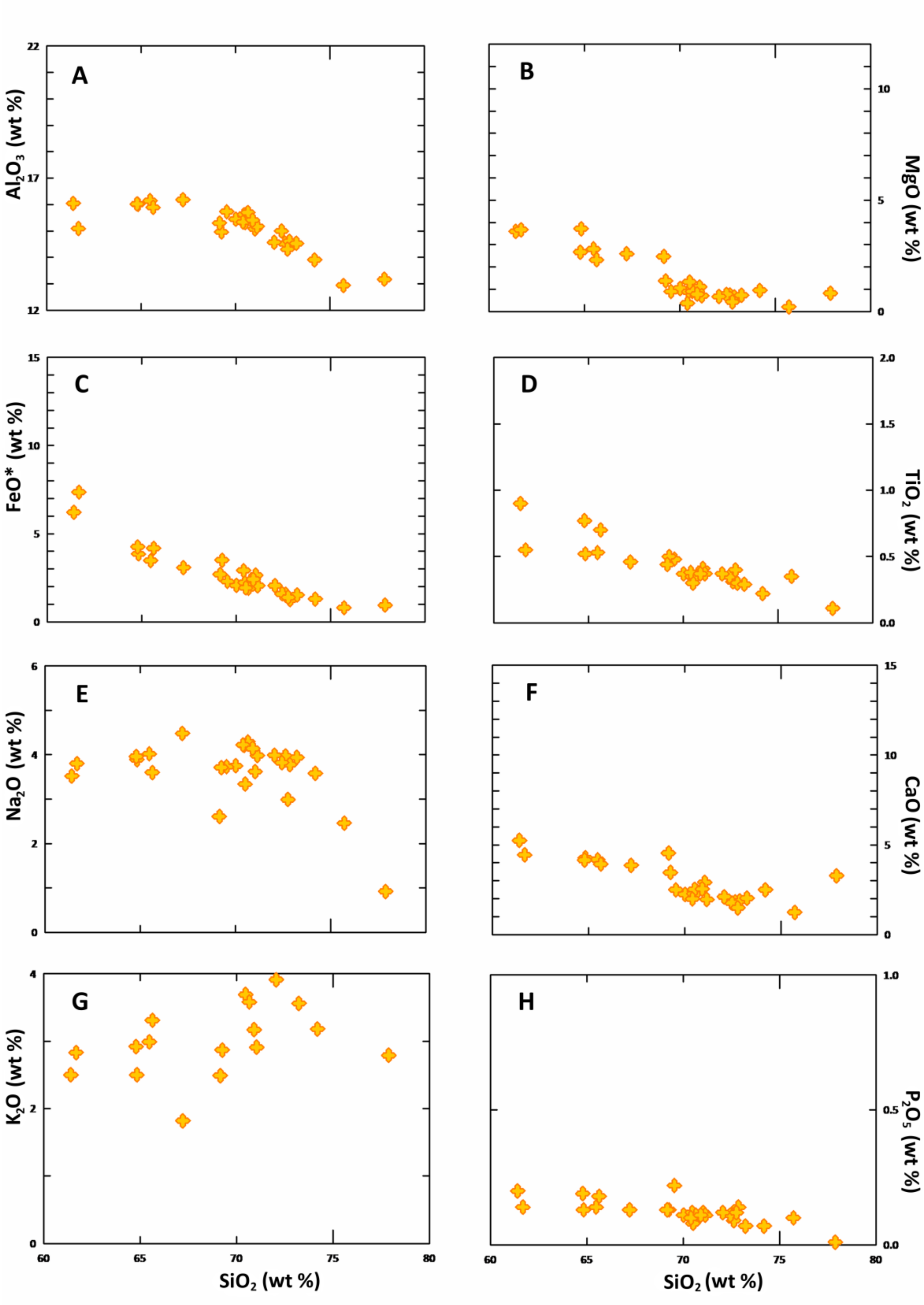

Figure 2.11 - Major element versus silica variation diagrams of the Lowland Creek volcanic province (Dudás et al., 2010; Scarberry, 2019).

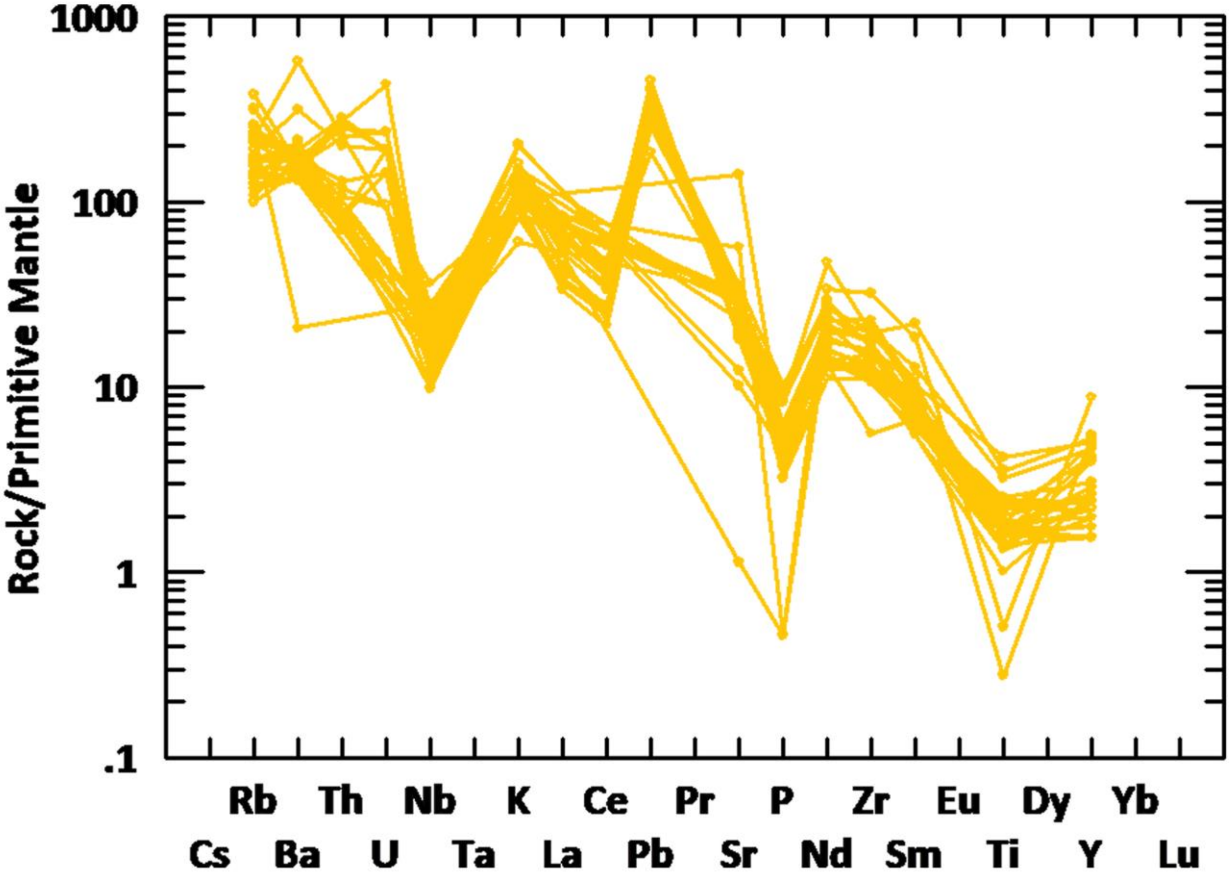

Figure 2.12 - Primitive mantle-normalized multi-element diagram using the normalization of Sun and McDonough (1989) for the Lowland Creek volcanic province (Dudás et al., 2010; Scarberry, 2019).

Chapter 3 - Background of Regional Porphyry Mineral Systems

3.1 Introduction

Porphyry ore systems originate from high-temperature magmatic hydrothermal fluids and are called "porphyry deposits" because of the porphyritic texture of the mineralized intrusions (Pirajno, 2009). Porphyry Cu ± Mo ± Au deposits are intrusion centered and are formed at ~1 to 7-km-depth, by fluids exsolved from magmas emplaced at ~5 to 15-km-deep in the upper crust (Richards, 2009; Park et al., 2021). The ore zones in porphyry deposits are a thick-walled, inverted "cup" over the parent intrusion (Amdt et al., 2015). Most known deposits are genetically related to intermediate to felsic (52 - 77 wt% SiO_2) calc-alkaline magmas in volcanic arcs (Richards, 2003; Richards, 2009; Ridley, 2013). Copper porphyry deposits are directly linked to the petrogenesis of arc magmas, and derive their fundamental characteristics (e.g., relatively high oxidation state and enrichment in alkalies, S, Cl, H_2O, metals, and metalloids) from subduction processes and metal(loid)-rich lithospheric mantle (Richards, 2003; Richards, 2009).

Arc magmas area enriched in H_2O, Cl, S and moderately oxidized (ΔFMQ = +1 to +2) relative to most other mantle derived magmas (ΔFMQ ≤ 0) (Richards, 2021). These magmas are predominantly formed by partial melting of the metasomatized wedge of asthenospheric mantle (Richards, 2003; Richards, 2009). Although magmas with these characteristics most commonly form directly in response to inputs from the subduction zone, it is also possible to extract compositionally and isotopically similar magmas from upper plate lithosphere that has been modified by prior subduction processes (Richards, 2009). Crustal thickness influences porphyry mineralization through volume of magmatic activity, timing of sulfide saturation, chalcophile element fertility and emplacement depth (Park et al., 2021). Thick crust (> 40 km) can influence and create the necessary conditions for porphyry Cu deposits, while thin crust (< 40 km) increases Au-rich porphyry Cu ore formation (Richards, 2003; Holwell et al., 2019; Park et al., 2021). Thick crust can also force deep crystallization of garnet-bearing cumulates that drive the oxidation associated with Cu mobilization and porphyry Cu deposits (Lee & Tang, 2020); much of this crystallization occurs at the base of the crust in MASH (e.g., melting-assimilation-storage-hybridization) zones (Hildreth & Moorbath, 1988; Richards, 2003). Garnet will preferentially incorporate Fe^{2+}, thus the resultant magma becomes enriched in Fe^{3+}, and more oxidized. The higher oxidation state leads to sulfide oxidation, where Cu is liberated into magmatic fluids (Lee & Tang, 2020). High La/Yb and Sr/Y ratios in arc magmas most likely reflect deep crustal garnet fractionation (as well as possible amphibole stability and melting of deep crustal plagioclase), with Yb and Y being compatible in garnet (Lee & Tang, 2020). As a result, Sr/Y and (Eu/Eu*)/Yb, another trace element ratio indicative of deep crustal magma fractionation have been utilized as proxies for Cu-fertility in magmas (Loucks, 2021). In this scheme, Sr/Y > 35 and (Eu/Eu*)/Yb > 2 reflect Cu-fertile magmas, while Sr/Y < 35 and (Eu/Eu*)/Yb < 2 characterize Cu-infertile magmas (Loucks, 2021; Lamont et al., submitted).

Porphyry Cu deposit formation is likely influenced and controlled by repeating, short-lived (e.g., ~3 m.y.) magmatic and hydrothermal injections (Mercer et al., 2015). The location of Cu porphyry systems (and coeval volcanic localizations) in the crust also appears to be partially controlled by fault systems, which act to focus coeval magmatism and porphyry-system development. For example, inherited trans-lithospheric fault systems apparently control the location of Au-rich Cu porphyry systems along the Central and South America Cordillera margin (Farrar et al., 2023; Wiemer et al., 2023).

As the magmas ascend into the upper crust, evolved melt further crystallizes and depressurizes, resulting in exsolution of dissolved volatiles which can either be brought to the surface through volcanic eruptions, fumarolic emissions, or form subsurface hydrothermal systems (Richards, 2021). Metal(loid)s dissolved in the magma preferentially partition into the magmatic fluids, resulting in their precipitation into economic porphyry, epithermal, and skarn deposits enriched in Cu, Mo, Au, and other similarly volatile elements (Richards, 2009; Saunders & Brueseke, 2011; Richards, 2021). Some porphyry deposits were also apparently formed from hydrous magmas derived by partial remelting of the metasomatized lithospheric roots and hydrous cumulate zones of former arc systems, as well as in regions devoid of volcanism but characterized by overthickened crust and lower-mid-crustal anatexis (Richards, 2009; Lamont et al., submitted). In the former, these systems are inferred to be in response to a variety of mechanisms that might generate magmatism, such as lithospheric thickening and thermal rebound, subcontinental lithospheric mantle delamination, or lithospheric extension (Richards, 2009). In the latter, the Cu-porphyry mineralization has been suggested to result from previously enriched (in metals and metalloids) mafic and felsic lower crustal rocks that then undergo crustal melting, generating metal(loid)-rich metals and ultimately porphyry Cu-systems (Lamont et al., submitted).

While porphyry Cu-systems generally have predominantly mantle sources, porphyry Mo-systems can be contributed by a subducting slab or lithospheric crust (Seedorff et al., 2005). Arc-related porphyry Mo-systems form in similar tectonic environments as many porphyry Cu-systems, and are considered to be an end-member or transitional spectrum of porphyry Cu-Systems (Taylor et al., 2012). The alkali-feldspar rhyolite-granite porphyry Mo-systems, or Climax type Mo-systems, formed in extensional environments (Taylor et al., 2012).

3.2 Absaroka Porphyry Mineral Systems

Mineralization associated with the Absaroka volcanic province generally occurs as disseminations and stockwork in intensely altered rock, and in fractures and veins that transect both mineralized intrusives and vent-series wall rocks (Hausel, 1982). Cu, Mo, and trace Au occupy the central portion of the provinces porphyry complexes and give way to Zn, Pb, and Ag ores laterally away from the centers of the complexes (Hausel, 1982). The primary districts and mineralized intrusives in the Absaroka volcanic province lie along a prominent north- northwest structural trend located several miles east of the Yellowstone National Park border (Figure 3.1) (Hausel, 1982), but overall effectively align with both different belts of Absaroka volcanoes (Chadwick, 1971).

The 54 – 52 Ma Washburn Group only contains one primary area of mineralization, the New World-Cooke City district, which lies on the Montana Wyoming border (Figure 3.1) (Hausel, 1982). The 50 – 48 Ma Sunlight Group contains three primary centers of mineralization and consists of the Sunlight, Eagle Creek, and Clouds Home Peak mineralized areas (Figure 3.1) (Hausel, 1982). The 47 – 44 Ma Thorofare Creek Group contains the greatest number of mineralized areas of the AVP, hosting the Kirwin-Wood River, Yellow Ridge, Birthday, Stinking Water, Robinson Creek, and Silver Creek mineralized areas (Figure 3.1) (Hausel, 1982).

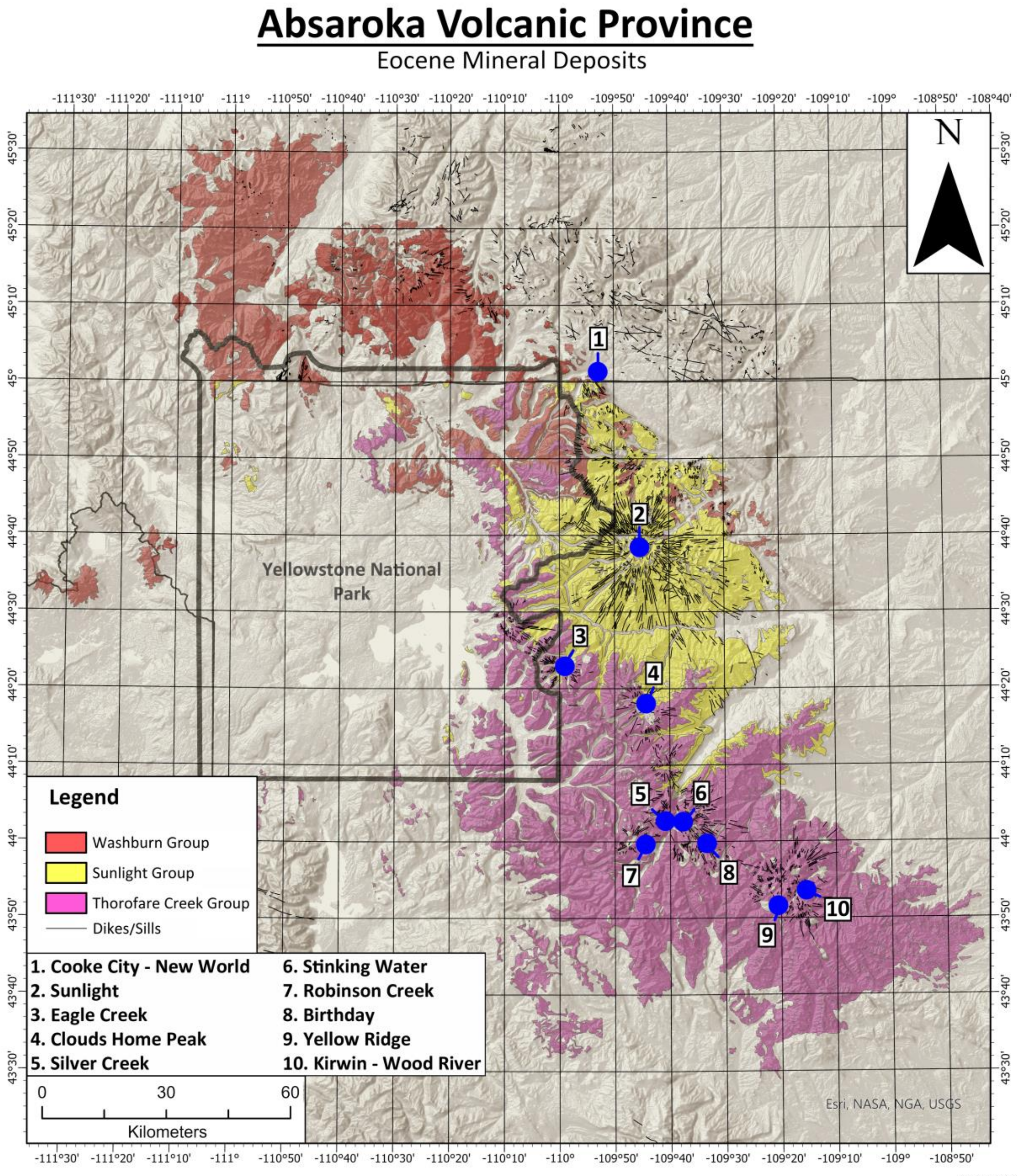

Figure 3.1 - Regional map of the major mineralized areas of the Eocene Absaroka Volcanic Province, divided into the 54 – 52 Ma Washburn group, the 50 – 48 Ma Sunlight group, and the 47 – 44 Ma Thorofare Creek group. Yellowstone National Park is outlined in black for reference location. Blue dots represent the locations of the major Cu-porphyry systems (Hausel, 1982; Vuke et al., 2013; Wyoming State Geological Survey, 2013; U.S. Geological Survey, 2013; U.S. Geological Survey, 2023). Notice how the Cu-porphyry systems are intimately linked to Absaroka stratovolcanoes and hypabyssal dike swarms.

3.3 Challis Porphyry Mineral Systems

The dominant porphyry systems within the central Idaho Challis volcanic province are Eocene molybdenum dominated porphyry mineralized systems, where Mo is the principal potentially economic product (Worthington, 2007). While porphyry Cu is present within the province, the region is primarily dominated by Mo porphyry systems (Whitney, 1975; Worthington, 2007). The Tertiary porphyry deposits within the central Idaho Challis volcanic province are post-Laramide, upper Paleocene to Eocene (55 – 36 Ma), which includes a large area of the Sawtooth batholith and two major deposits in the Idaho porphyry belt (Worthington, 2007). The Idaho porphyry belt is a northeast trending linear zone of rhyolite dikes, mostly within the Idaho batholith (Worthington, 2007).

The two main deposits within the Idaho porphyry belt include the Little Falls and CUMO deposits located in Boise County, Idaho (Worthington, 2007). These deposits consist of northeast trending rhyolite dikes that cut the Idaho batholith with siliceous pyritic zones containing molybdenite and Cu-bearing minerals in thin quartz veins (Whitney, 1975; Worthington, 2007). The Red Mountain prospect and the Walton deposit are located within Custer County, Idaho (Worthington, 2007). The deposits consist of quartz stockworks and veins containing molybdenite in Eocene granite (Worthington, 2007). The White Mountain prospect is similar and occupies the same small stock as the Walton deposit (Worthington, 2007). Other Mo-rich deposits include the West Eight Mile deposit, Ima deposit, and Rocky Bar District, which all host molybdenite associated with either small dikes or mineralized stocks (Worthington, 2007).

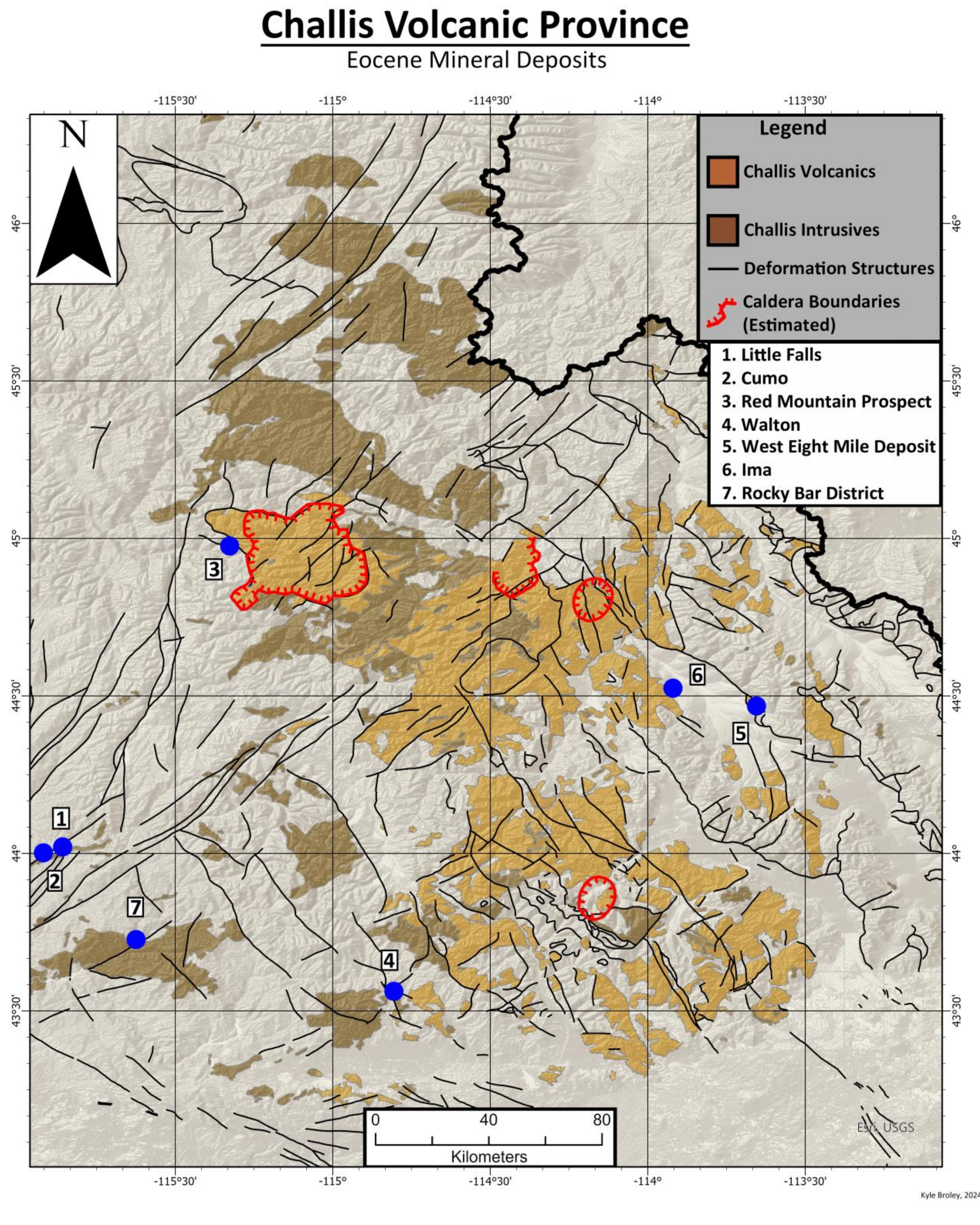

Figure 3.2 - Regional map of the Eocene Challis volcanic province, divided into the Challis volcanics and Challis Intrusives showing caldera boundaries, regional deformation structures, and areas of Eocene mineralization. Blue dots represent the locations of the major mineralization (Worthington, 2007; Lewis et al., 2012; Vuke et al., 2013; U.S. Geological Survey, 2019; U.S. Geological Survey, 2022; U.S. Geological Survey, 2023).

3.4 Lowland Creek Porphyry Mineral Systems

Evaluation of the Lowland Creek volcanic province indicates that the upper ash-flow tuff sequence erupted from a caldera (Foster, 1987). In the Lowland Creek volcanic province, Eocene epithermal precious metal systems are present and formed in response to caldera formation and accompanying hydrothermal system development (Foster, 1987). These include the Ruby mine (and associated prospects), the Tuxedo and Flume Gulch mines, and the Montana Tunnels gold deposit (Foster, 1987. No apparent porphyry mineralization is associated with the Lowland Creek volcanic province.

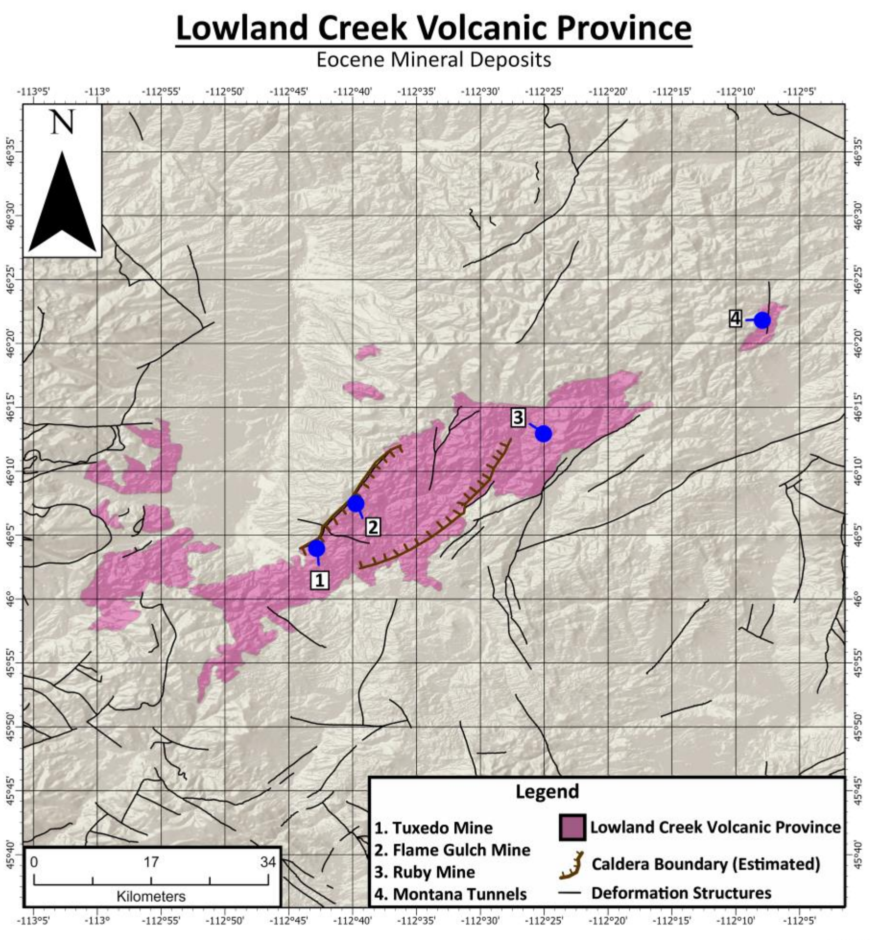

Figure 3.3 - Regional map of the Eocene Lowland Creek volcanic province showing local deformation structures, caldera boundary, and mining locations. Blue dots represent the locations of the major mineralization (Foster, 1987; Vuke et al., 2013; U.S. Geological Survey, 2013).

Chapter 4 - Methods

The mapping of volcanic provinces and porphyry mineral systems plays a crucial role in this study, providing visual identification of trends in the emplacement of these units. Shapefile, raster, and vector datasets were acquired from Idaho, Montana, and Wyoming state geological surveys and state organizations, as well as the United States Geological Survey (USGS), to create all maps in this study (Appendix A). Available raster datasets were merged and converted into hillshade using ESRI ArcGIS Pro before being overlayed with shapefiles of state boundaries collected from the state organizations, and the Absaroka, Challis, and Lowland Creek volcanic provinces collected from 500,000 and 100,000 scale geologic map shapefiles from the respective state geologic surveys. Geospatial data points for known mines and mine claims of Eocene porphyry mineral systems were downloaded from the state geological surveys and the USGS. These shapefile points were overlayed on the created maps to identify associated trends between these systems and the regional volcanic provinces.

Raw Absaroka, central Idaho Challis, and Lowland Creek volcanic provinces' geochemical data were compiled from relevant literature and online databases. A total of 248 whole rock major and trace element analyses make up the sample suite used in this study. The Absaroka volcanic province is divided by the province Supergroup members with 67 samples for the Washburn Group (5 taken from Hiza (1999); 46 taken from Feeley et al. (2001);16 taken from Lindsay & Feely (2003)), 35 samples for the Sunlight Group (8 taken from Hiza (1999); 27 taken from Feeley (2003)), and 10 samples for the Thorofare Creek Group (taken from Hiza (1999)) for a total of sample suite of 112. The central Idaho Challis province consists of 108 samples divided into Challis intrusives (8 samples taken from Gaschnig et al. (2011)) and Challis volcanics (100 samples taken from McKervey (1998)). The Lowland Creek volcanic province samples suite consists of 28 samples (13 samples taken from Dudás et al. (2010); 15 samples taken from Scarberry (2019)). In all the major element data collected, iron was presented as either FeO^T or $Fe_2O_3^T$ and was adjusted to the ratio of FeO and Fe_2O_3 using the Le Maitre (1976) method for volcanic rocks (data used can be found in the supplemental file). With the ratio between FeO and Fe_2O_3 determined, the major element data was recalculated to anhydrous.

Literature and data on regional porphyry mineral systems were compiled from available literature. A total of 21 regional mineralized areas are examined in this study. A total of 10 Eocene age mineralized areas for the Absaroka volcanic province are taken from Hausel (1982). A total of 7 mineralized areas for the central Idaho Challis volcanics are taken from Worthington (2007). A total of 4 mineralized areas for the Lowland Creek volcanic province are taken from Foster (1987). The information shows locations of mines and claims, ore and igneous geochronology, and the region's associated mineralization of ore systems within the Absaroka, central Idaho Challis, and Lowland Creek volcanic provinces.

Chapter 5 - Results and Discussion

5.1 Results

The Absaroka volcanic province consists of basaltic to rhyolitic stratovolcanoes, shield volcanoes, and dike swarms which erupted between 54 – 44 Ma (Figure 5.1). The northwest-trending belt erupted through the 170 km-thick lithosphere of the Wyoming Craton. The central Idaho Challis volcanic province is comprised of basaltic andesite to rhyolite fissure vent and caldera eruptions that occurred between ~50 – 44 Ma (Figure 5.1). The Lowland Creek volcanic province formed due to trachyandesite to rhyolitic caldera eruptions between 53 – 49 Ma (Figure 5.1). The Challis and Lowland Creek volcanics erupted through thinner (90 – 120 km-thick) lithosphere.

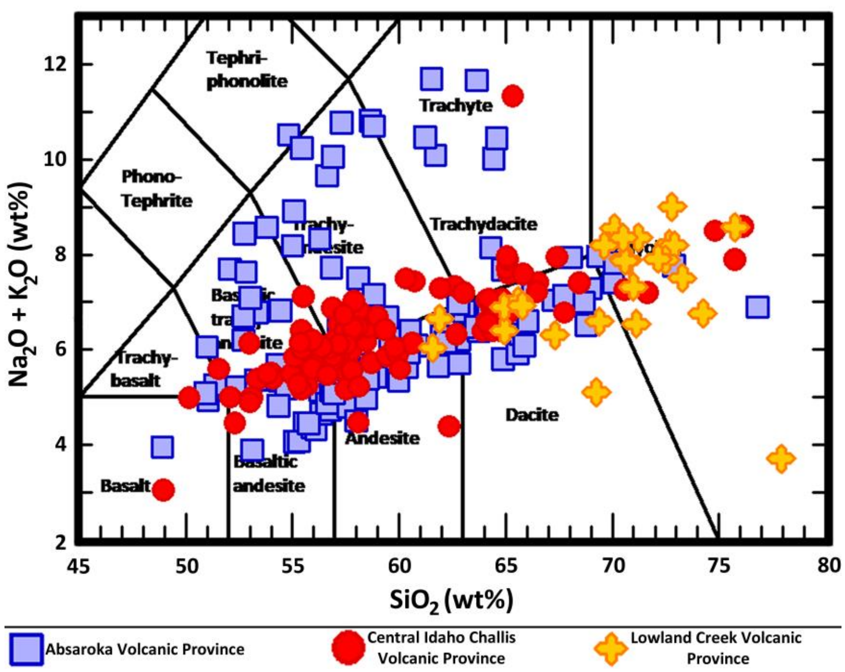

Figure 5.1 - Comparative total alkali versus silica diagram for the Absaroka (blue squares), central Idaho Challis (red circles), and Lowland Creek volcanic provinces (yellow crosses) with the Le Maitre et al., (1989) classification grid (Absaroka data: Hiza, 1999; Feeley et al., 2002; Lindsay & Feeley, 2003) (Challis data: Norman & Mertzman, 1991; McKervey, 1998; Gaschnig et al., 2011) (Lowland Creek data: Dudás et al., 2010; Scarberry, 2019).

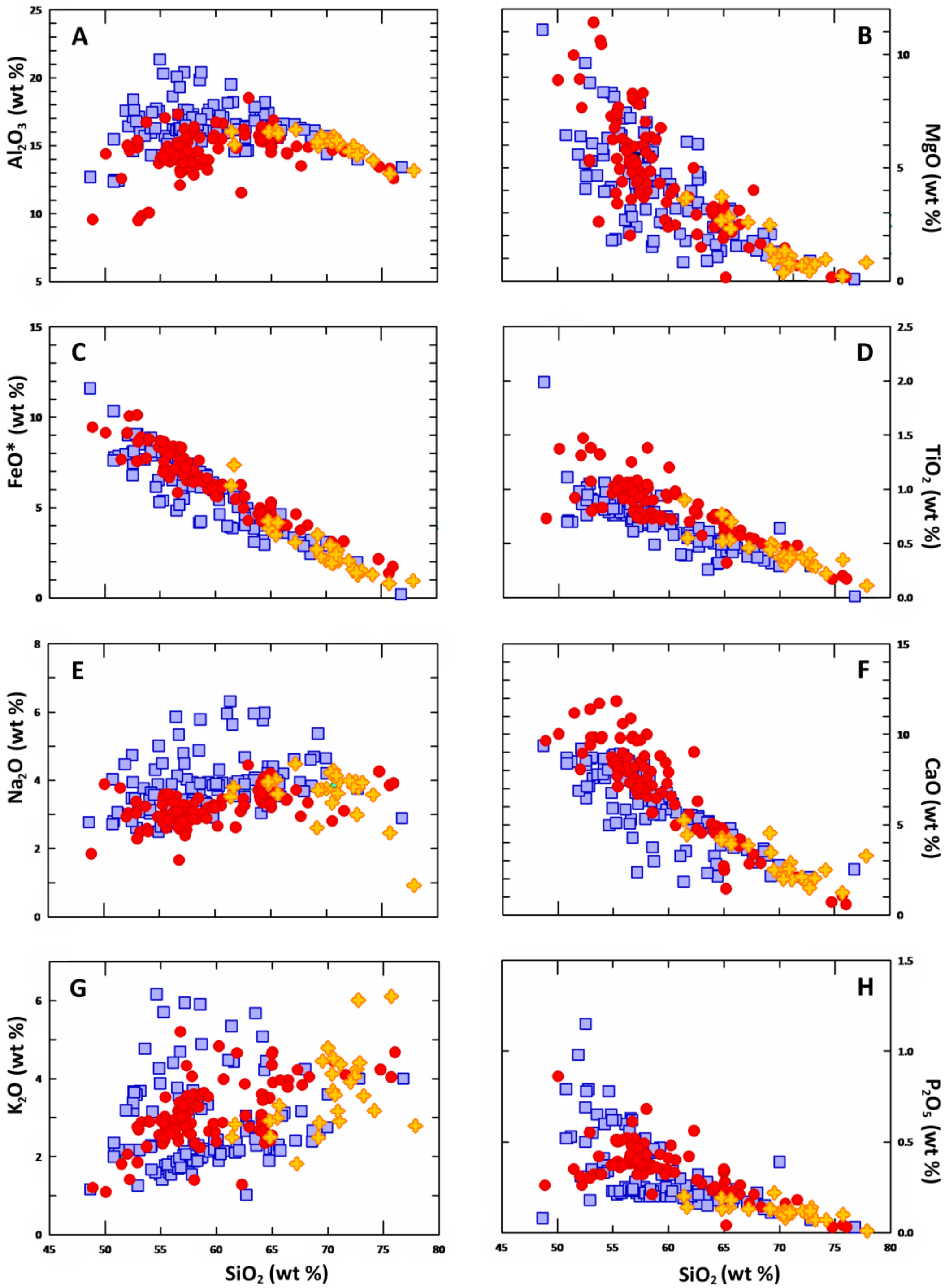

Figure 5.2 - Comparative major element versus silica variation diagrams of the Absaroka, central Idaho Challis, and Lowland Creek volcanic provinces (symbols same as in Figure 5.1) (Absaroka data: Hiza, 1999; Feeley et al., 2002; Lindsay & Feeley, 2003) (Challis data: Norman & Mertzman, 1991; McKervey, 1998; Gaschnig et al., 2011) (Lowland Creek data: Dudás et al., 2010; Scarberry, 2019).

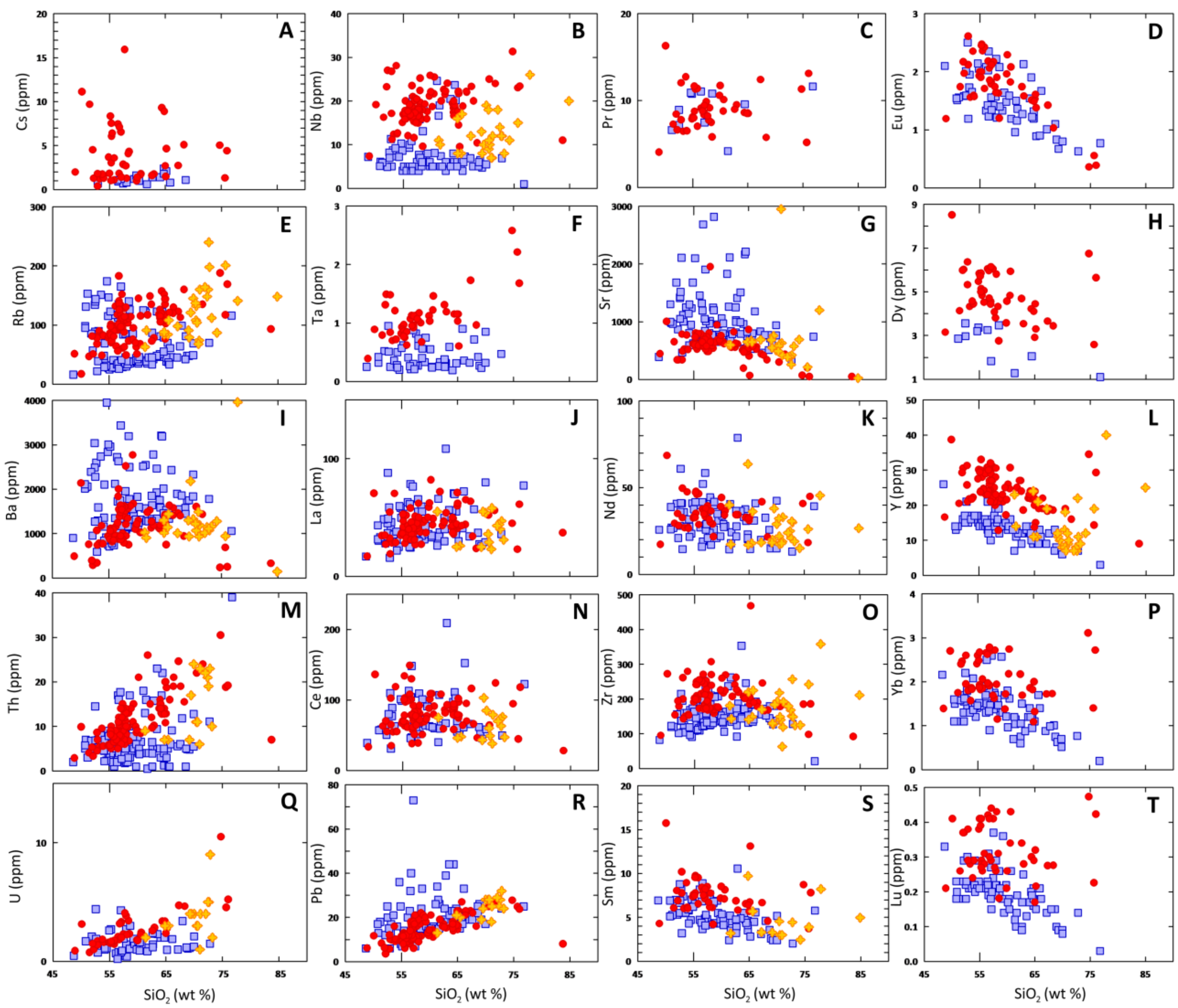

Figure 5.3 - Comparative trace element versus silica diagrams for the Absaroka, central Idaho Challis, and Lowland Creek volcanics (symbols same as in Figure 5.1) (Absaroka data: Hiza, 1999; Feeley et al., 2002; Lindsay & Feeley, 2003) (Challis data: Norman & Mertzman, 1991; McKervey, 1998; Gaschnig et al., 2011) (Lowland Creek data: Dudás et al., 2010; Scarberry, 2019).

Comparative major element diagrams for the Absaroka, central Idaho Challis, and Lowland Creek volcanic provinces show strong negative arrays for wt% FeO*, TiO_2, and CaO vs. wt% SiO_2 and slightly more scattered arrays for wt% MgO and P_2O_5 vs. wt% SiO_2 that decrease compared to an increase in wt% SiO_2 (Figure 5.2). All three volcanic provinces show variable increases of wt% K_2O and Na_2O in a scattered array with increasing wt% SiO_2 (Figure 5.2). The Absaroka and central Idaho Challis volcanic provinces show an array with an increase in wt% Al_2O_3 between 45 – 65 wt% SiO_2 before transitioning to a decreasing array that matches with the Lowland Creek volcanic province for wt% SiO_2 contents greater than ~65 wt% (Figure 5.2).

The variation in trace element concentrations vs. SiO2 is shown in Figure 5.3 for all three provinces. The diagrams show that trends in enrichment and depletion relative to wt% SiO_2 are similar for all three localities for SiO_2 concentrations between 45 – 77 wt% SiO_2. All three volcanic provinces show similar general patterns of enrichment in LILE and depletion of HFSE compared to primitive mantle (Figure 5.4). The Absaroka volcanic province shows more depletion in Th, Nb, Zr, Ti, Y, Yb, and Lu and more enrichment in U and Pb compared to the central Idaho Challis and Lowland Creek volcanic province (Figure 5.3; Figure 5.4). The central Idaho Challis volcanic province shows more enrichment in Cs, La, Nd, Zr, Sm, Eu, and Dy compared to the Absaroka and Lowland Creek volcanic provinces (Figure 5.3; Figure 5.4). The comparative primitive mantle-normalized diagram for all three provinces follows similar enrichment and depletion trends between 45 – 77 wt% SiO_2 with some anomalous enrichment in the more silica-rich samples. The Lowland Creek volcanic province shows more depletion in Ba and Sr compared to the Absaroka and central Idaho Challis volcanic provinces in the primitive mantle-normalized diagram, but Ba and Sr concentrations decrease with increasing wt% SiO_2 for both the Absaroka and central Idaho Challis volcanic province (Figure 5.3; Figure 5.4).

The major mineral systems associated with the Absaroka volcanic province consist of Cu-dominated porphyry deposits that spatially are linked to the same north-northwestern trend of the Absaroka volcanoes (e.g., Absaroka Cu-porphyry systems are only found where eroded stratovolcanoes exist). In a plot of Sr/Y versus wt% SiO_2 (Figure 5.5A) the Absaroka volcanics lie predominantly within the porphyry Cu-fertile zone of Loucks (2021), having a range of Sr/Y values between 27.2 to 247.3 and a mean value of 77.1. The lowest Sr/Y values for the Absaroka volcanics are from the samples taken from the Washburn Group, while the highest values are from the Thorofare Creek Group. The Absaroka volcanics also plot within the Cu-fertile magma region on the Sr/Y versus (Eu/Eu*)/Yb diagram (Figure 5.4B), having Sr/Y > 35 and (Eu/Eu*)/Yb > 2.

In contrast, the central Idaho Challis volcanics contain Mo-dominant porphyry mineral systems throughout the province, with rare occurrences of W-Cu porphyry systems. These volcanics have Sr/Y values that are predominantly < 35, ranging from 1.7 to 69.7 and having a mean value of 24.9, plotting within the porphyry Cu-infertile region of the Sr/Y vs. SiO2 diagram (Figure 5.4A). The Sr/Y vs. (Eu/Eu*)/Yb (Figure 5.4B) values for the central Idaho Challis volcanic province sample suite follow the same pattern. The zones of mineralization for the central Idaho Challis volcanic province are situated mainly around the vent facies of the province.

The Lowland Creek volcanics have Sr/Y values ranging from 0.96 to 245.8, with a mean value of 53.2 (Figure 5.4A). Despite having values within the porphyry Cu-fertile range on the Sr/Y vs. SiO_2 diagram, the Lowland Creek volcanic province is not known to contain any Eocene porphyry mineral systems.

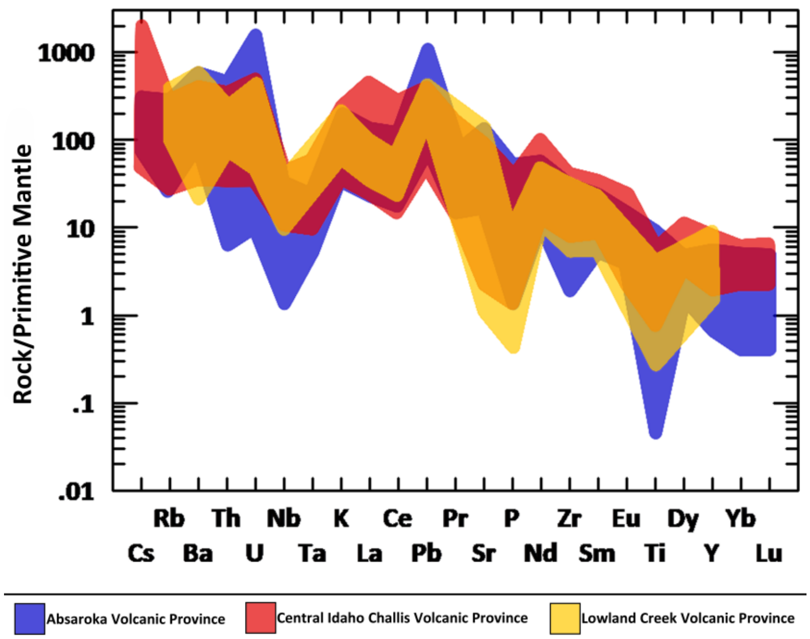

Figure 5.4 – Primitive-mantle-normalized multi-element diagram using the normalization of Sun and McDonough (1989) (Absaroka data: Hiza, 1999; Feeley et al., 2002; Lindsay & Feeley, 2003) (Challis data: Norman & Mertzman, 1991; McKervey, 1998; Gaschnig et al., 2011) (Lowland Creek data: Dudás et al., 2010; Scarberry, 2019).

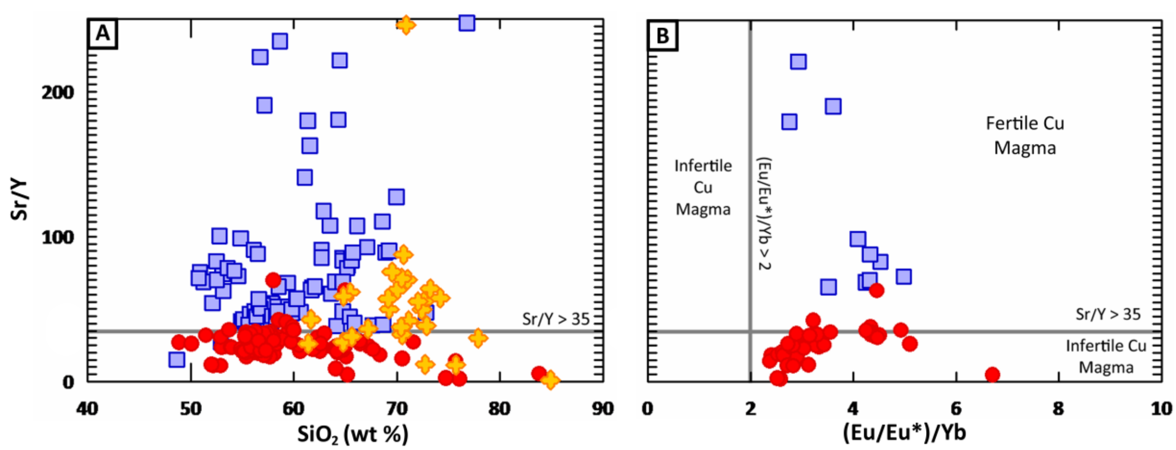

Figure 5.5 - (A) Sr/Y versus wt% SiO_2 comparative diagram for the Absaroka, central Idaho Challis, and Lowland Creek volcanic province with the boundary for porphyry Cu-fertile magmas defined by Loucks, (2021) and Lamont et al. (submitted). (B) Sr/Y versus (Eu/Eu*)/Yb comparative diagram for available samples of the Absaroka and central Idaho Challis volcanic province using the fertile Cu-magma boundaries defined by Loucks (2021) and Lamont et al., (submitted). Symbols same as Figure 5.1. (Absaroka data: Hiza, 1999; Feeley et al., 2002; Lindsay & Feeley, 2003) (Challis data: Norman & Mertzman, 1991; McKervey, 1998; Gaschnig et al., 2011) (Lowland Creek data: Dudás et al., 2010; Scarberry, 2019).

5.2 Discussion

The mineralization associated with each of the volcanic provinces provides additional insight into their tectonomagmatic origin. The Cu-dominant porphyry systems associated with the Absaroka volcanic province follow the generally accepted style of formation within an arc or arc-like environment based on the models of Richards (2009; -2021). The Sr/Y vs. wt% SiO_2 and Sr/Y vs. (Eu/Eu*)/Yb diagrams support the arc-like genesis for the Absaroka volcanic province (Figure 5.5). The timeline for Cu-porphyry system development proposed by Mercer et al. (2014) , further supports this theory, with the Absaroka volcanic province having multiple phases of volcanism over a few Mya timescale (Figure 5.6) that would resupply metals and provide a resurgence of heat for continued hydrothermal activity necessary for porphyry Cu development. In contrast, the central Idaho Challis volcanic province is dominated by porphyry Mo-systems and its Sr/Y vs. (Eu/Eu*)/Yb characteristics also align with a lack of Cu-porphyry systems, supporting the tectonomagmatic context that the central Idaho Challis volcanic province formed in an extensional environment, unrelated to subduction/compressional tectonics. The Lowland Creek volcanic province sample suite shows a decrease in Sr/Y as wt% SiO_2 concentrations increases, suggesting that rocks in the province with more intermediate compositions could, potentially, host porphyry deposits. However, the Lowland Creek volcanic province is also not characterized by stratovolcano formation and was only active for a duration of ~4 Myr, neither of which are ideal for Cu-porphyry mineralization (Mercer et al., 2014; Richards, 2021).

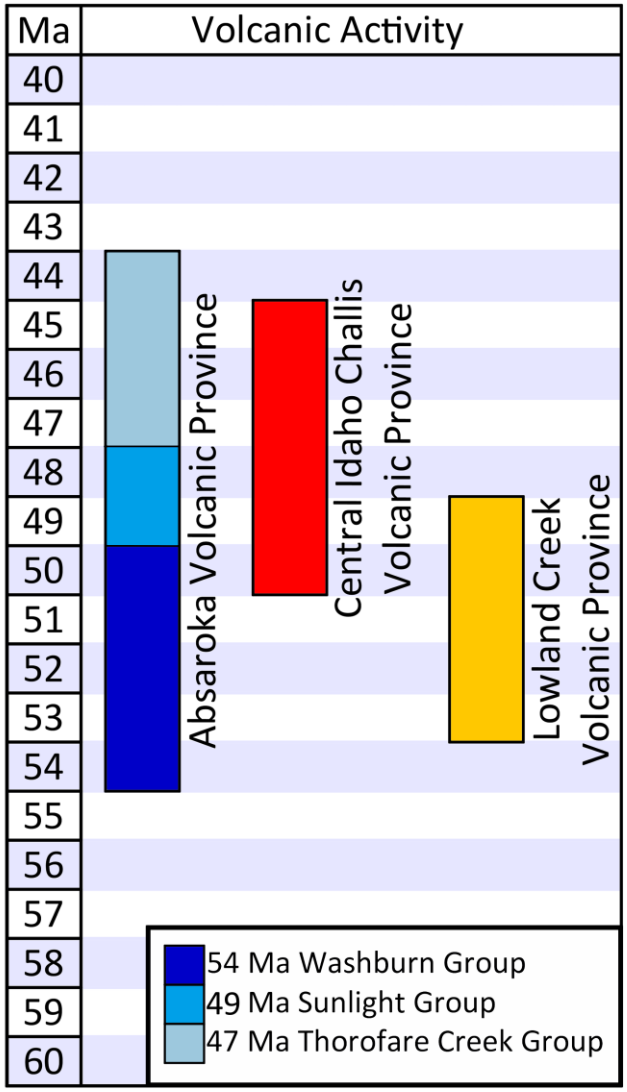

Figure 5.6 - Graph showing the timeline of regional volcanism, including the division of the Washburn, Sunlight, and Thorofare Creek Groups of the Absaroka volcanic province (Absaroka data: Hiza, 1999; Feeley et al., 2002; Lindsay & Feeley, 2003) (Challis data: Norman & Mertzman, 1991; McKervey, 1998; Gaschnig et al., 2011) (Lowland Creek data: Dudás et al., 2010; Scarberry, 2019).

5.2.2. Regional Tectonics and central Idaho Challis-Absaroka volcanism

There are three major tectonic models used to describe the tectonomagmatic origin for the Challis-Absaroka volcanism. The tectonic model of Dostal and Jutras (2021) is focused on slab failure of the Farallon plate occurring because of a subduction blockage by the most buoyant portion of Siletzia, coupled with lithospheric weaking induced by the Yellowstone hotspot (e.g., Siletzia "source"), and transtensional faulting caused by oblique subduction of the Juan de Fuca plate beneath the Cascadia subduction zone. The tectonic model of Feeley (2003) shows initial flat slab subduction of the Farallon plate before a separation occurs further west that supplies upwelling asthenosphere, as the slab founders away from the continental lithosphere. Both models, based on detailed Sr-Nd-Pb isotope studies of the Absaroka province by Feeley (2003), also show that Absaroka magmas were sourced either in the Archean lithospheric mantle, or at the base of that mantle (e.g., a substantial ancient lithospheric component in Absaroka magmas). The model discussed by Breitsprecher et al. (2003) is based on a northwest-southeastern slab tear creating a window that supplies the upwelling asthenosphere necessary for the formation of the central Idaho Challis and Absaroka volcanic provinces. The tectonic models developed for this study consider these previously developed models but is significantly different because it also includes the porphyry mineral systems and their constraints on possible sources of magmas, and thus tectonomagmatic origin.

5.2.1. Proposed Tectonic Models for the Absaroka-Challis-Lowland Creek Volcanic Provinces

Prior to the Farallon plate contacting the Wyoming craton, compressional tectonics and subduction aided the creation of the Sevier fold-thrust belt and the Laramide orogeny. As the shallowly subducting, and eastward moving Farallon plate contacted the lithosphere of the 170-km-thick, westward moving, Wyoming Craton. At, or perhaps just before this contact, the thick North American lithosphere would have induced mantle-flow-related hydrodynamic (viscous) "suction" (O/Driscoll et al., 2009; Manea et al., 2012; Benowitz & Mann, in press) in the underlying mantle wedge, which acts to keep underlying slabs at shallow dips under continental lithosphere (e.g., van Hunen et al., 2004; Manea & Gurnis, 2007; Rodriguez-González et al., 2012; -2014). Hydrodynamic "suction" has been documented in settings characterized with (e.g., van Hunen et al., 2004; Benowitz & Mann, in press) and without (e.g., Manea & Gurnis, 2007; O'Driscoll et al., 2009; Manea et al., 2009; Rodriguez-González et al., 2012; -2014) the presence of subducting oceanic plateaus or overthickened lithosphere. Thus, it is applicable to our model for Absaroka-Challis-Lowland Creek volcanism, regardless of whether an oceanic plateau, like the conjugate Shatsky rise, was subducted under North America. We estimate that sometime around 55 Ma (Figure 5.7), a tear or break formed in the slab due to sudden variations in the depth of subduction. It is possible that this tear could have been induced as the subducting slab impacted existing basal topography of the Wyoming craton or previously subducted material under the craton (Klepeis et al., 2019). The timing of this tear correlates with the ending of the Laramide orogeny and likely corresponds physically to the "big break" imaged by Sigloch et al. (2008) and Sigloch (2011), between older and deeper segments of the geophysically imaged Farallon slab that lie under North America (e.g., "Laramide Slab"), and the currently subducting slab.

As the subducting Farallon plate contacted the Wyoming Craton, the angle of subduction was altered and changed from shallow to steeper subduction underneath and shallow- to shallower-slab subduction west of the Wyoming craton. the subduction angle underneath the Wyoming craton allowed for melt generation and the formation of a belt of arc-like volcanoes, the Absaroka volcanic province (e.g., the Absaroka Arc), beginning at 54 Ma. This slight steepening of a shallow slab is not unique and currently is present under the Trans-Mexico volcanic belt (Arce et al., 2020). Under the Wyoming craton in the Eocene, the slab would have stayed in the 130 ± 70 km depth threshold for arc magma generation and melt production (Isacks & Barazangi et al., 1977; England et al., 2004; Syracuse & Abers, 2006; van Kekan et al., 2011). Edge driven convection effects along the western edge of the Wyoming craton would have acted to focus melts upward and help to explain the localization of the Absaroka Arc and why this arc-like magmatism was not more laterally widespread (King & Anderson, 1998; Jadamec & Billen, 2010; Kaislaiemi & van Hunen, 2014; Brueseke et al., 2019). Similarly, more diffuse slab edge-driven upwelling to the east and north, has been proposed to explain the widespread alkaline magmatism in Montana, Wyoming, and South Dakota (Duke, 2009; Duke et al., 2014). Melts would have also been focused through the Wyoming craton lithosphere, as suggested by Chadwick (1970), along lithospheric fault systems like what has been documented in other volcanic arcs (Rabiee et al., 2020; Farrar et al., 2023; Benowitz & Mann, in press).

The northwestward tearing (breaking), and the resulting sudden variation in the depth of subduction of the Farallon plate at the northwestern edge of the Wyoming craton provided the necessary conditions for the formation of the Lowland Creek volcanic province at 53 Ma. At ~50 Ma (Figure 5.8), the shallowly subducting Farallon plate detached from the subcontinental lithospheric mantle west of the Wyoming craton, likely due to the initial docking and insertion of Siletzia further to the west along the Cordilleran margin at 51 Ma (Figure 1.2), which initiated a localized magmatic flare-up (e.g., ~52 – 46 Ma "Breakoff Belt" magmatism in Washington; Tepper et al., 2023) and regional extension (Humphreys, 2009; Schmandt & Humphreys, 2011; Wells et al., 2014; Eddy et al., 2017; Tepper & Clark, 2024).

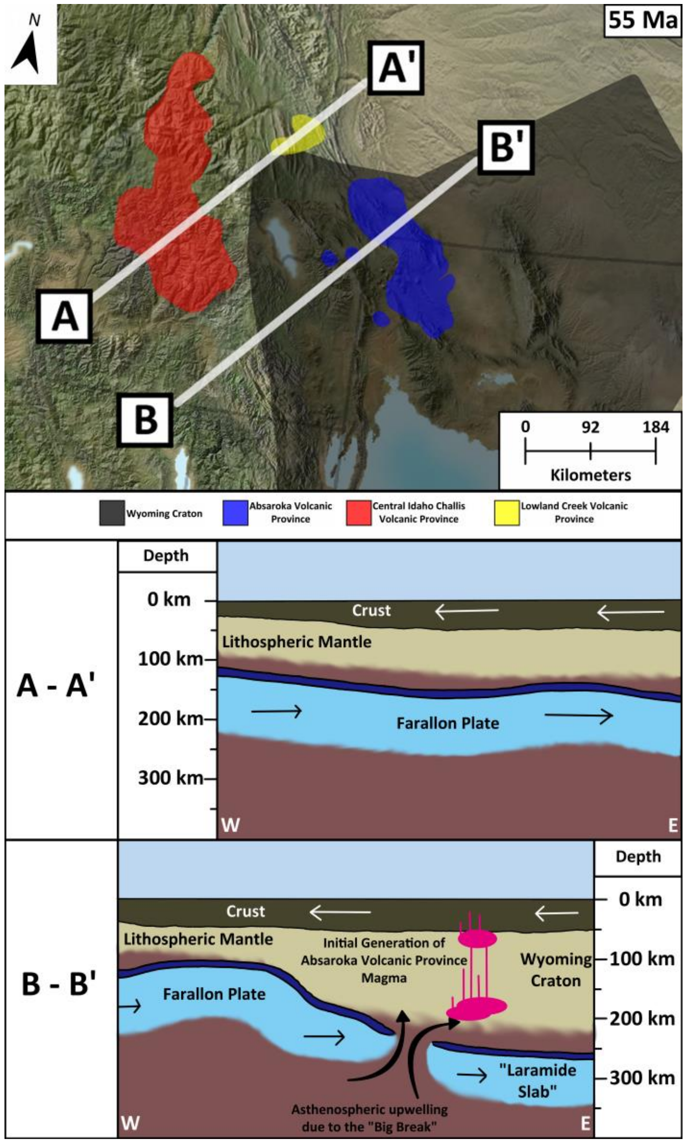

Figure 5.7 – Tectonic model for 55 Ma. (A - A') Shallow subduction of the Farallon plate underneath the region of the central Idaho Challis and Lowland Creek volcanic provinces. (B – B') Contact with the Wyoming craton initiated the "Big Break" (Sigloch et al., 2008; Sigloch, 2011) separating the Farallon plate from the "Laramide slab."

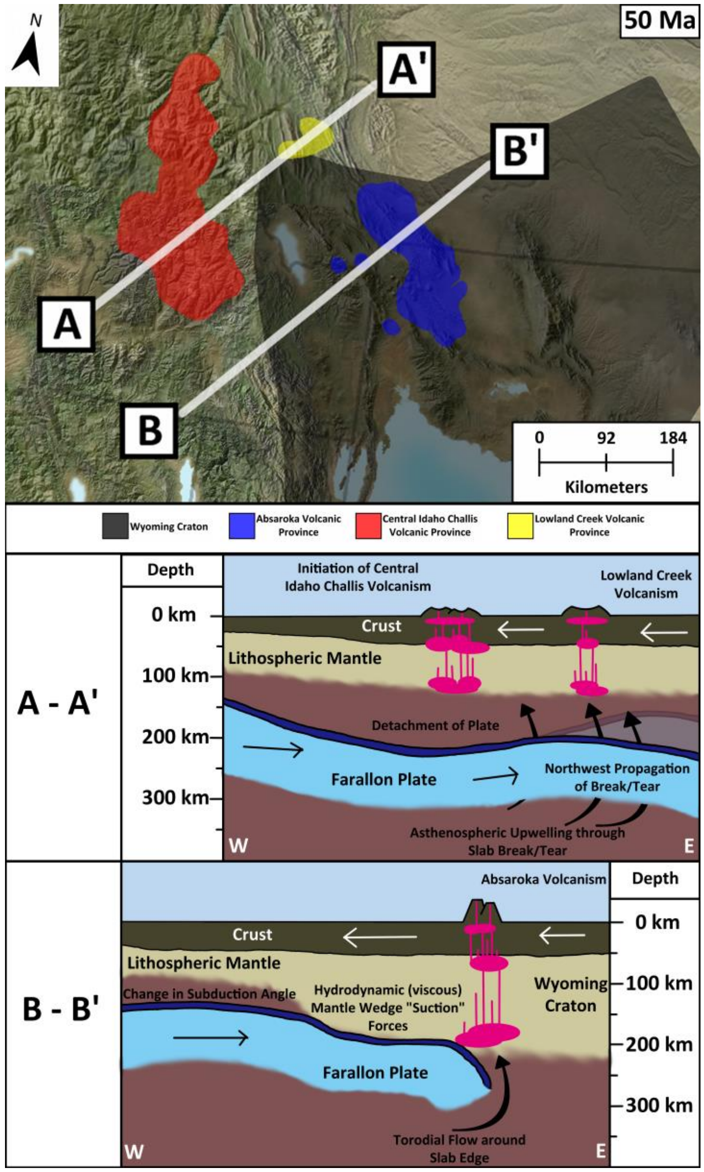

Figure 5.8 – Tectonic model for 50 Ma. (A – A’) Slab tear propagates north and west as Farallon detachment occurred west and northwest of the Wyoming craton. (B – B’) Steepening of subduction angle and hydrodynamic (mantle wedge “suction” force under the Wyoming craton, coupled with toroidal flow around the slab edge, triggered subduction and Absaroka Arc magmatism.

As the detached Farallon plate began to founder, extension across the region west of the Wyoming craton allowed for the formation of Challis volcanism due to channelized flow of asthenosphere between the lithosphere and the Farallon plate (Dostal & Jutras, 2021). Underneath the craton, the arc-like subduction dynamics continued, and it is likely that focused mantle flow along the craton margin started to destroy the craton (e.g., Crow et al., 2011; Cooper et al., 2021), providing more lithospheric contributions to the Absaroka magmatism. The docking of Siletzia along the western margin of North America was completed by 49 Ma (Eddy et al., 2017), concurrent with the end of the Lowland Creek volcanic province. As extension continued, input from the toroidal flow focused along the foundering Farallon plate diminished, and the central Idaho Challis volcanic province ceased magmatism at ~45 Ma. As this segment of the Farallon plate foundered beneath the craton (Figure 5.9) (Sigloch et al., 2008; Sigloch, 2011) and rolled back to the south (Humphreys, 1995; Humphreys, 2009). Absaroka Arc magmatism ended ca. ~44 Ma.

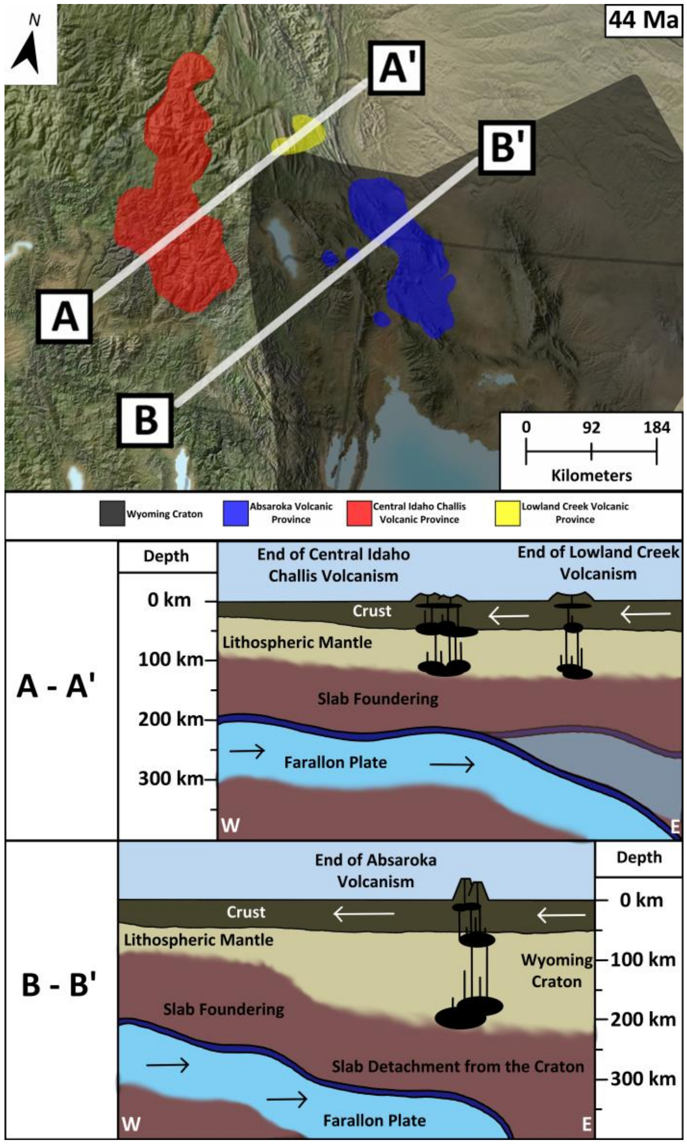

Figure 5.9 – Tectonic model for 44 Ma. (A – A') Slab foundering occurred underneath the region of the central Idaho Challis and Lowland Creek volcanic provinces. (B – B') Farallon plate detaches from underneath the craton.

Chapter 6 - Conclusions

1) The Absaroka volcanic province was formed through subduction processes occurring around a slab edge, adjacent to the western margin of the Wyoming Craton. Notable lithospheric components identified in the geochemistry of the Absaroka volcanics can be attributed to interaction with the lithosphere as the magma made its way through the 170-km-thick Wyoming craton or from melting of the subcontinental lithospheric mantle in response to asthenospheric melts emplaced at the lithosphere-asthenosphere boundary, in response to the change in subduction angle of the Farallon plate. The presence of Cu-dominated porphyry deposits within the Absaroka volcanic province, coupled with the Sr/Y-SiO_2 and Sr/Y-(Eu/Eu*)/Yb geochemistry (e.g., Cu-fertile magma), and the occurrence of the Cu-porphyry deposits centered on stratovolcanoes that would have resembled those of the modern Cascades, also suggests an arc origin for the Absaroka volcanic province. Absaroka magmas and related Cu-porphyry systems were emplaced and formed along lithosphere-scale fault corridors, that must reflect inherited structures in the Wyoming craton lithosphere. We also suggest that the hydrodynamic (viscous) mantle wedge "suction" forces of the Wyoming craton led to, or at a minimum, helped facilitate, shallow slab subduction at the western edge of the Wyoming craton. When the slab broke ca. ~55 Ma, Absaroka arc volcanism initiated at the dangling slab edge. Absaroka arc volcanism ended after Siletzia was fully accreted at 49 Ma.
2) The central Idaho Challis volcanic province was formed through extensional processes caused by delamination and foundering of the ancestral Farallon plate (e.g., Laramide slab) after the hydrodynamic (viscous) mantle wedge "suction" forces of the plate under the

Wyoming province and additional strain brought about by the docking of Siletzia at ca. ~51 - 49 Ma. The abundance of Mo-dominant porphyry mineral systems and a lack of Cu-dominant porphyry mineral systems supports an extensional environment for the formation of the central Idaho Challis volcanics. Geochemical variations of the Challis volcanics in the Sr/Y vs. SiO_2 and Sr/Y vs. (Eu/Eu*)/Yb geochemistry of Challis magmas support this theory, with the central Idaho Challis volcanic province plotting predominantly in the Cu-infertile magmas region of the Cu-fertility discrimination diagram.

3) The Lowland Creek volcanic province was likely formed due to a combination of uneven subduction, related to the tearing (breaking) of the Farallon plate as it subducted under the Wyoming Craton to the south and southeast, and slab-window or slab-edge toroidal flow around the foundering Laramide slab. While available Sr/Y data shows a variable depletion with increasing wt% SiO2, additional geochemical studies need to be conducted to better understand the formation of the Lowland Creek volcanic province.

4) Porphyry mineralized systems associated with magmatism in complex tectonic environments are useful for helping to clarify the tectonism that dominates in a specific location (e.g., subduction vs. extension). The combination of economically significant mineral deposits, geological, and geochemical data allows for the creation of a complex tectonic model necessary to understand the tectonomagmatic origins of the Absaroka, central Idaho Challis, and Lowland Creek volcanic province. The subduction processes of the Laramide slab under this region were dynamic. The processes consisted of a change in the angle of subduction leading to the hydrodynamic (viscous) mantle wedge "suction" forces of the Farallon plate under the Wyoming Craton. To the west of this region, the Laramide slab is presumed to have foundered in response to these forces and release of the

plate under the Wyoming Craton, and/or strain induced by the docking of Siletzia to the western margin of North America.

5) Additional work is still needed to align the tectonomagmatic model discussed here, with geodynamic models of the region during the Eocene. To fully understand the complexity of this region, there is a need for isotopic and additional geochemical data for the volcanic provinces, especially the central Idaho Challis and the Lowland Creek volcanic province.

References

Arce, J.L., Ferrari, L., Morales-Casique, E., Vasquez-Serrano, A., Arroyo, S.M., Layer, P.W., Benowitz, J., and Lopez-Martinez, M., 2020, Early Miocene arc volcanism in the Mexico City Basin: inception of the Trans-Mexican volcanic belt: Journal of Volcanology and Geothermal Research, v. 408, p. 107104.

Anderson, M.L., Blakely, R.J., Wells, R.E., and Dragovich, J.D. 2024, Deep structure of Siletzia in the Puget Lowland: Imaging an obducted plateau and accretionary thrust belt with potentialfields:Tectonics,v.43, e2022TC007720.https://doi.org/10.1029/2022TC007720

Appel, M., 2002, Alkaline and peraluminous intrusives in the Clarno Formation around Mitchell, Oregon: ramifications on magma genesis and subduction tectonics [M.S. thesis]: Corvallis, Oregon State University, 222p.

Arndt, N., and Ganino, C., 2012, Metals and Society (L. D. Meinert, Ed.): Berlin, Heidelberg, Springer Berlin Heidelberg, doi:10.1007/978-3-642-22996-1.

Armstrong, R.L., and Ward, P., 1991, Evolving geographic patterns of Cenozoic magmatism in the North American Cordillera: the temporal and spatial association of magmatism and metamorphic core complexes: Journal of Geophysical Research, v. 96, doi:10.1029/91jb00412.

Bedrosian, P.A., and Frost, C.D., 2023, Geophysical extent of the Wyoming Province, western USA: Insights into ancient subduction and craton stability: Bulletin of the Geological Society of America, v. 135, p. 725–742, doi:10.1130/B36417.1.

Benowitz, J.A. and Mann, M.E., in press, Inherited Upper-plate Controls On Localized Arc Magmatism Since ca. 100 Ma along the Alaska Range Suture Zone: Tectonics and seismicity of Alaska and Western Canada: Earthscope and beyond, p. 1 – 48.

Best, M.G., Christiansen, E.H., de Silva, S., and Lipman, P.W., 2016, Slab-rollback ignimbrite flareups in the southern Great Basin and other Cenozoic American arcs: A distinct style of arc volcanism: Geosphere, v. 12, p. 1097–1135, doi:10.1130/GES01285.1.

Bestland, E.A., Hammond, P.E., Blackwell, D.L.S., Kays, M.A., Retalack, G.J., Stimac, J., 2002, Geologic Framework of the Clarno Unit, John Day Fossil Beds National Monument, Central Oregon: Oregon Department of Geology and Mineral Industries OFR-O-02-03, 39p.

Breitsprecher, K., Thorkelson, D.J., Groome, W.G., and Dostal, J., 2003, Geochemical confirmation of the Kula-Farallon slab window beneath the Pacific Northwest in Eocene time: Geology, v. 31, p. 351–354, doi:10.1130/00917613(2003)031<0351:GCOTKF>2.0.CO;2.

Brueseke, M.E., Benowitz, J.A., Trop, J.M., Davis, K.N., Berkelhammer, S.E., Layer, P.W., and Morter, B.K., 2019, The Alaska Wrangell Arc: ~30 Ma of subduction-related magmatism along a still active arc-transform junction: Terra Nova, v. 31, p. 59–66, doi:10.1111/ter.12369.

Camp, V.E., Ross, M.E., Duncan, R.A., and Kim-brough, D.L., 2017, Uplift, rupture, and rollback of the Farallon slab reflected in volcanic perturbations along the Yellowstone adakite hot spot track: Journal of Geophysical Research, v. 122, p. 7009–7041, https://doi.org/10.1002/2017JB014517.

Carrapa, B., DeCelles, P.G., and Romero, M., 2019, Early Inception of the Laramide Orogeny in Southwestern Montana and Northern Wyoming: Implications for Models of Flat-Slab Subduction: Journal of Geophysical Research: Solid Earth, v. 124, p. 2102–2123, doi:10.1029/2018JB016888.

Chadwick, R.A., 1970, Belts of eruptive centers in the Absaroka-Gallatin volcanic province, Wyoming-Montana: Geol. Soc. Am. Bull., v. 81, p. 267-274.

Colgan, J.P., Egger, A.E., John, D.A., Cousens, B., Fleck, R.J., and Henry, C.D., 2011, Oligocene and Miocene arc volcanism in northeastern California: Evidence for post-Eocene segmentation of the subducting Farallon plate: Geosphere, v. 7, p. 733–755, doi:10.1130/GES00650.1.

Coney, P.J., 1978, Mesozoic–Cenozoic Cordilleran plate tectonics, in Smith, R.B., and Eaton, G.P., eds., Cenozoic Tectonics and Regional Geophysics of the Western Cordillera: Geological Society of America Memoir 152, p. 33–50, doi: 10 .1130 /MEM152 -p33 .

Coney, P.J., and Reynolds, S.J., 1977, Cordilleran Benioff zones: Nature, v. 270, p. 403–406, doi:10.1038/270403a0.

Constenius, K.N., 1996, Late Paleogene extensional collapse of the Cordilleran foreland fold and thrust belt: Geol. Soc. Am. Bull., v. 108, p. 20-39.

Constenius, K.N., Esser, R.P., and Layer, P.W., 2003, Extensional collapse of the Charleston-Nebo Salient and its relationship to space-time variations in Cordilleran orogenic belt tectonism and continental stratigraphy: Cenozoic Systems of the Rocky Mountain region, p. 303–343.

Cooper, C.M., Farrington, R.J., and Miller, M.S., 2021, On the destructive tendencies of cratons: Geology, v. 49, p. 195–200, doi:10.1130/G48111.1.

Copeland, P., Currie, C.A., Lawton, T.F., and Murphy, M.A., 2017, Location, location, location: The variable lifespan of the Laramide orogeny: Geology, v. 45, p. 223-226, https://doi.org/10.1130/G38810.1

Crow, R., Karlstrom, K.E., Asmeron, Y., Schmandt, B., Polyak, V., DuFrane, S.A., 2011, Shrinking of the Colorado Plateau via lithospheric mantle erosion: evidence from Nd and Sr isotopes and geochronology of Neogene basalts: Geology, v. 39, p. 27-30.

DeCelles, P. G., 2004, Late Jurassic to Eocene evolution of the Cordilleran thrust belt and foreland basin system, western U.S.A, Am. J. Sci., 304, 105–168, doi:10.2475/ajs.304.2.105.

Dickinson, W.R., 2004, Evolution of the North American Cordillera, Annual Review of Earth and Planetary Sciences, Vol. 32, 13-45, doi:10.1146/32.101802.120257.

Dickinson, W. R., M. A. Klute, J. Michael, S. U. Janecke, E. R. Lundin, M. A. McKittrick, and M. D. Olivares, 1988, Paleogeographic and paleotectonic setting of Laramide sedimentary basins in the central Rock Mountains region, Geol. Soc. Am. Bull., 100, 1023–1039, doi:10.1130/ 0016-7606(1988)1002.3.CO;2.

Dostal, J., and Jutras, P., 2021, Tectonic and petrogenetic settings of the Eocene Challis-Kamloops volcanic belt of western Canada and the northwestern United States: International Geology Review, v. 00, p. 1–19, doi:10.1080/00206814.2021.1992800.

Dostal, J., Breitsprecher, K., Church, B.N., Thorkelson, D., and Hamilton, T.S., 2003, Eocene melting of Precambrian lithospheric mantle: Analcime-bearing volcanic rocks from the Challis-Kamloops belt of south central British Columbia: Journal of Volcanology and Geothermal Research, v. 126, p. 303–326, doi:10.1016/S0377-0273(03)00153-7.

du Bray, E., Aleinikoff, J.N., and Lund, K., 2012, Synthesis of Petrographic, Geochemical, and Isotopic Data for the Boulder Batholith, Southwest Montana: U. S. Geological Survey Professional Paper, v. 1793.

Dudás, F.Ö., and Harlan, S.J., 1999, An Ancient Depleted Mantle Sample from a 42-Ma Dike in Montana: Constraints on Persistence of the Lithosphere during Eocene Magmatism: Journal of Geology, v. 107, p. 287-299.

Dudás, F.Ö., Ispolatov, V.O., Harlan, S.S., and Snee, L.W., 2010, 40Ar/39Ar geochronology and geochemical reconnaissance of the Eocene Lowland Creek volcanic field, west-central Montana: Journal of Geology, v. 118, p. 295–304, doi:10.1086/651523.

Duke, I.G., 2009, Black Hills–Alberta carbonatite–kimberlite linear trend: Slab edge at depth: Tectonophysics, v. 464, p. 186-194

Duke, G.I., Carlson, R.W., Frost, C.D., Hearn, B.C., and Eby, G.N., 2014, Continent-scale linearity of kimberlite–carbonatite magmatism, mid-continent North America: Earth and Planetary Science Letters, v. 403, p. 1–14, doi:10.1016/j.epsl.2014.06.023.

Eddy, M.P., Clark, K.P., and Polenz, M., 2017, Age and volcanic stratigraphy of the Eocene Siletzia oceanic plateau in Washington and on Vancouver Island: Lithosphere, v.9, p.652–664,https://doi.org/10.1130/L650.1

England, P., Engdahl, R., and Thatcher, W., 2004, Systematic variation in the depths of slabs beneath arc volcanes: Geophysical Journal International, v. 156 (2), p. 377-408, https://doi.org/10.1111/j.1363-246X.2003.02132.x.

Erslev, E.A., Worthington, L.L., Anderson, M.L., and Miller, K.C., 2022, Laramide crustal detachment in the Rockies: Cordilleran shortening of fluid-weakened foreland crust: Rocky Mountain Geology, v. 57, p. 65–97, doi:10.24872/rmgjournal.57.2.65.

Farrar, A.D., Cooke, D.R., Hronsky, J.M.A., Wood, D.G., Benavides, S.B., Cracknell, M.J., Banyard, J.F., Gigola, S., Ireland, T., Jones, S.M., Piquer, J., 2023, A Model for the Lithospheric Architecture of the Central Andes and the Localization of Giant Porphyry Copper Deposit Clusters: Economic Geology, v. 118 (6), p. 1235-1259, doi:10.5382/econgeo.5010.

Feeley, T.C., 2003, Origin and tectonic implications of across-strike geochemical variations in the Eocene Absaroka Volcanic Province, United States: Journal of Geology, v. 111, p. 329–346, doi:10.1086/373972.

Feeley, T.C., and Cosca, M.A., 2003, Time vs. composition trends of magmatism at Sunlight volcano, Absaroka volcanic province, Wyoming: Bulletin of the Geological Society of America, v. 115, p. 714–728, doi:10.1130/0016-7606(2003)115<0714:TVCTOM>2.0.CO;2.

Feeley, T.C., Cosca, M.A., and Lindsay, C.R., 2002, Petrogenesis and implications of calc-alkaline cryptic hybrid magmas from Washburn volcano, Absaroka Volcanic Province, USA: Journal of Petrology, v. 43, p. 663–703, doi:10.1093/petrology/43.4.663.

Foster, F., 1987, Epithermal precious-metal systems associated with an Eocene Cauldron: Lowland Creek Volcanic Field, southwestern Montana: Montana Bureau of Mines and Geology Special Publication, v. 95, p. 53–54.

Foster, D.A., Mueller, P.A., Mogk, D.W., Wooden, J.L., and Vogl, J.J., 2006, Proterozoic evolution of the western margin of the Wyoming craton: Implications for the tectonic and magmatic evolution of the northern Rocky Mountains: Canadian Journal of Earth Sciences, v. 43, p. 1601–1619, doi:10.1139/E06-052.

Fritz, W.J., 1982, Geology of the Lamar River Formation northeast of Yellowstone National Park: Wyoming Geological Association Guidebook, Thirty-third annual field conference – 1982, p. 73-101

Gaschnig, R.M., Vervoort, J.D., Lewis, R.S., and Tikoff, B., 2011, Isotopic evolution of the Idaho batholith and Challis intrusive province, Northern US Cordillera: Journal of Petrology, v. 52, p. 2397–2429, doi:10.1093/petrology/egr050.

Glazner, A.F., 2022, Cenozoic magmatism and plate tectonics in western North America: Have we got it wrong? Special Paper of the Geological Society of America, v. 553, p. 95–108, doi:10.1130/2021.2553(09).

Hausel, W., 1982, General geologic setting and mineralization of the porphyry copper deposits, Absaroka volcanic plateau, Wyoming: Guidebook - Wyoming Geological Association, v. 33, p. 297–313.

Heller, P.L., and Liu, L., 2016, Dynamic topography and vertical motion of the U.S. Rocky Mountain region prior to and during the Laramide orogeny: Bulletin of the Geological Society of America, v. 128, p. 973–988, doi:10.1130/B31431.1.

Hildreth, W., and Moorbath, S., 1988, Crustal contributions to arc magmatism in the Andes of central Chile: Contributions to Mineralogy and Petrology, v. 98, p. 455-489.

Hiza, M.M., 1999, The geochemistry and geochronology of the Eocene Absaroka volcanic province, northern Wyoming and southwest Montana, USA [Ph.D. Thesis]: Oregon State University, 243 p.

Holwell, D.A., Fiorentini, M., McDonald, I., Lu, Y., Giuliani, A., Smith, D.J., Keith, M., and Locmelis, M., 2019, A metasomatized lithospheric mantle control on the metallogenic signature of post-subduction magmatism: Nature Communications, v. 10, p. 1–10, doi:10.1038/s41467-019-11065-4.

Howlett, C.J., Reynolds, A.N., and Laskowski, A.K., 2021, Magmatism and Extension in the Anaconda Metamorphic Core Complex of Western Montana and Relation to Regional Tectonics: Tectonics, v. 40, p. 104–116, doi:10.1029/2020TC006431.

Humphreys, E., 2009, Relation of flat subduction to magmatism and deformation in the western United States: Memoir of the Geological Society of America, v. 204, p. 85–98, doi:10.1130/2009.1204(04).

Humphreys, E.D., and Grunder, A.L., 2022, Tectonic controls on the origin and segmentation of the Cascade Arc, USA: Bulletin of Volcanology, v. 84, p. 1–13, doi:10.1007/s00445-022-01611-2.

Isacks, B.L., and Barazangi, M., 1977, Geometry of Benioff zones: Lateral segmentation and downwards bending of the subducted lithosphere: Island Arcs, Deep Sea Trenches, and Back-Arc Basins, v. 1, p. 99-114.

Iyer, H.M., Hitchcock, T., 1989, Upper mantle velocity structure in continental U.S. and Canada. In: Pakiser, L.C., Mooney, W.D. (Eds.), Geophysical Framework of the Continental United States. Geological Society of America Memoir, vol. 172, pp. 249 – 284. Boulder, CO.

Jackson, W.T., McKay, M.P., Bartholomew, M.J., Allison, D.T., Spurgeon, D.L., Shaulis, B., VanTongeren, J.A., and Setera, J.B., 2019, Initial Laramide tectonism recorded by upper cretaceous paleoseismites in the northern Bighorn Basin, USA: Field indicators of an applied end load stress: Geology, v. 47, p. 1059–1063, doi:10.1130/G46738.1.

Jadamac, M.A., and Billen, M.I., 2010, Reconciling surface plate motions with rapid three-dimensional mantle flow around a slab edge: Nature, v. 485 (7296), p. 338-341.

Janecke, S.U., and Snee, L.W., 1993, Timing and episodicity of Middle Eocene volcanism and onset of conglomerate deposition, Idaho: Journal of Geology, v. 101, p. 603–621, doi:10.1086/648252.

Janecke, S.U., Hammond, B.F., Snee, L.W., and Geissman, J.W., 1997, Rapid extension in an Eocene volcanic arc: Structure and paleogeography of an intra-arc half graben in central Idaho: Bulletin of the Geological Society of America, v. 109, p. 253–267, doi:10.1130/0016-7606(1997)109<0253:REIAEV>2.3.CO;2.

Kaislaniemi, L., and van Hunen, J., 2014, Dynamics of lithospheric thinning and mantle melting by edge-driven convection: Application to Moroccan Atlas Mountains: Geochemistry, Geophysics, Geosystems, v. 15, p. 3175-3189, https://doi.org/10.1002/2014GC005414.

King, S.D., and Anderson, D.L., 1998, Edge-driven convection: Earth and Planetary Science Letters, v. 160, p. 289-296.

Klepeis, K., Webb, L., Blatchford, H., Schwartz, J., Jongens, R., Tumbull, R., Stowell, H., 2019, Deep slab collision during Miocene subduction causes uplift along crustal scale reverse faults in Fjordland, New Zealand: GSA Today, v. 29, p. 4-10 https://doi.org/10.1130/gsatg399a.1.

Lageson, D.R., Kalakay, T.J., and Foster, D.A., 2022, Mountain Building: the Orogenic Evolution of Montana: MBMG Special Publication 122, v. Geology of, p. 1–65, https://www.mbmg.mtech.edu/.

Lamont, T., Loader, M., Museum, N.H., Roberts, N.M.W., Survey, B.G., and Cooper, F., 2024, The role of crustal anatexis in porphyry copper ore formation during flat-slab subduction : Insights from the Laramide Belt , SW USA The role of crustal anatexis in porphyry copper ore formation during flat-slab subduction : Insights from the Laramide Bel:, doi:10.31223/X5HH54.

Le Maitre, R.W., 1976, Contributions to Mineralogy and Petrology Some Problems of the Projection of Chemical Data into Mineralogical Classifications: Contributions to Mineralogy and Petrology, v. 189, p. 181–189.

Lee, C.T.A., and Tang, M., 2020, How to make porphyry copper deposits: Earth and Planetary Science Letters, v. 529, p. 115868, doi:10.1016/j.epsl.2019.115868.

Li, L., Fan, M., and Zhu, L., 2021, Early Oligocene Surface Uplift in Southwestern Montana During the North American Cordilleran Extension: Tectonics, v. 40, p. 1–17, doi:10.1029/2020TC006671.

Lindsay, C.R., and Feeley, T.C., 2003, Magmagenesis at the Eocene Electric Peak-Sepulcher Mountain complex, Absaroka Volcanic Province, USA: Lithos, v. 67, p. 53–76, doi:10.1016/S0024-4937(02)00252-9.

Liu, L., Gurnis, M., Seton, M., Saleeby, J., Müller, R.D., and Jackson, J.M., 2010, The role of oceanic plateau subduction in the Laramide orogeny: Nature Geoscience, v. 3, p. 353-357.

Lipman, P.W., Prostka, H.J., and Christiansen, R.L., 1972, Cenozoic volcanism and plate tectonic evolution of western United States: Part 1. Early and middle Cenozoic: Philosophical Transactions of the Royal Society of London, ser. A, v. 271, p. 217–248, doi: 10.1098/rsta.1972.0008.

Loucks, R., 2021, Deep entrapment of buoyant magmas by orogenic tectonic stress: Its role in producing continental crust, adakites, and porphyry copper deposits: Earth-Science Reviews, v. 220, p. 103744, https://doi.org/10.1016/j.earscirev.2021.103744.

Manea, V.C., Pérez-Gussinyé, M., and Manea, M., 2012, Chilean flat slab subduction controlled by overriding plate thickness and trench rollback: Geology, v. 40 (1), p. 35-38.

McKervey, John Antony, 1998, The petrogenesis of the Eocene Challis Volcanic Group, Idaho, western U.S.A. [Ph.D. thesis]: The Open University, 365 p.

Mercer, C.N., Reed, M.H., and Mercer, C.M., 2014, Time Scales of Porphyry Cu Deposit Formation : Insights from Titanium Diffusion in Quartz: v. 110, p. 587–602.

Norman, M.D., and Mertzman, S.A., 1991, Petrogenesis of Challis volcanics from central and southwestern Idaho: trace element and Pb isotopic evidence: Journal of Geophysical Research, v. 96, p. 13,279-13,293, doi:10.1029/91jb00285.

Norman, M.D., and Mertzman, S.A., 1991, Petrogenesis of Challis volcanics from central and southwestern Idaho: trace element and Pb isotopic evidence: Journal of Geophysical Research, v. 96, p. 13,279-13,293, doi:10.1029/91jb00285.

O'Drisocll, L.J., Humphreys, E.D., and Saucier, F., 2009, Subduction adjacent to deep continental roots: Enhanced negative pressure in the mantle wedge, mountain building and continental motion: Earth and Planetary Science Letters, v. 280 (1-4), p. 61-70.

Park, J., Campbell, I.H., Chiaradia, M., Hao, H., Lee, C., 2021, Crustal magmatic controls on the formation of porphyry copper deposits: Nature Review Earth & Environment, v. 2, p. 542 – 557, doi:10.1038/s43017-021-00182-8.

Pirajno, F., 2009, Hydrothermal Processes and Mineral Systems: Dordrecht, Springer Netherlands, 1–1250 p., doi:10.1007/978-1-4020-8613-7.

Prodehl, C., and Lipman, P.W., 1989, Chapter 14: Crustal structure of the Rocky Mountain region: Memoir of the Geological Society of America, v. 172, doi:10.1130/MEM172-p249.

Rabiee, A., Rossetti, F., Asahara, Y., Azizi, H., Lucci, F., Lustrino, M., and Nozaem, R., 2020, Long-lived, Eocene-Miocene stationary magmatism in NW Iran along a transform plate boundary: Gondwana Research, v. 85, p. 237-262.

Richards, J.P., 2003, Tectono-magmatic precursors for porphyry Cu-(Mo-Au) deposit formation: Economic Geology, v. 98 (8), p. 1515-1533.

Richards, J.P., 2009, Post-subduction porphyry Cu-Au and epithermal Au deposits: Products of remelting of subduction-modified lithosphere: Geology, v. 37, p. 247–250, doi:10.1130/G25451A.1.

Richards, J.P., 2022, Porphyry copper deposit formation in arcs: What are the odds? Geosphere, v. 18, p. 130–155, doi:10.1130/GES02086.1.

Ridley, J., 2013, Ore Deposit Geology: Cambridge University Press, doi:10.1017/CBO9781139135528.

Rodriguez-González, J., Billen, M.I., and Negredo, A.M., 2014, Non-steady-state subduction and trench-parallel flow induced by overriding plate structure: Earth and Planetary Science Letters, v. 401, p. 227-235.

Rodriguez-González, J., Negredo, A.M., and Billen, M.J., 2012, The role of the overriding plate thermal state on slab dip variability and on the occurrence of flat subduction: Geochemistry, Geophysics, Geosystems, v. 13 (1).

Sanford, R., 2005, Geology and Stratigraphy of the Challis Volcanic Group and Related Rocks, Little Wood River Area, South-Central Idaho: Geological Survey Bulletin 2064-11, 25 p., http://pubs.usgs.gov/bul/2064/ii/.

Saunders, J.A., and Brueseke, M.E., 2012, Volatility of metal(loids) during subduction-related "distillation" and the geochemistry of epithermal ores of western USA: Economic Geology, v. 107, p. 165 – 172.

Scarberry, K.C., Yakovlev, P. V, and Schwartz, T.M., 2011, Mesozoic Magmatism in Montana: MBMG Special Publication 122: Geology of Montana, v. 1, p. 30.

Schmandt, B., and Humphreys, E., 2011, Seismically imaged relict slab from the55 Ma Siletzia accretion to the northwest United States: Geology, v. 39, p. 175–178, https://doi.org/10.1130 /G31558.1.

Schwartz, T.M., and Schwartz, R.K., 2013, Paleogene post-compressional intermontane basin evolution along the frontal Cordilleran fold-and-thrust belt of southwestern Montana: Bulletin of the Geological Society of America, v. 125, p. 961–984, doi:10.1130/B30766.1.

Schwartz, T.M., Schwartz, R.K., and Weislogel, A.L., 2019, Orogenic Recycling of Detrital Zircons Characterizes Age Distributions of North American Cordilleran Strata: Tectonics, v. 38, p. 4320–4334, doi:10.1029/2019TC005810.

Seedorff, E., Dilles, J.H., Proffett, J.M., Einaudi, M.T., Zurcher, L., Stavast, W.J.A., Johnson, D.A., and Barton, M.D., 2005, Porphyry Deposits: Characteristics and Origin of Hypogene Features: Economic Geology, v. 100th Anni, p. 251–298.

Sigloch, K., 2011, Mantle provinces under North America from multifrequency: v. 12, p. 1–27, doi:10.1029/2010GC003421.

Sigloch, K., Quarrie, N.M.C., and Nolet, G., 2008, Two-stage subduction history under North America inferred from multiple-frequency tomography: Nature Geoscience, v. 1, p. 458–462, doi:10.1038/ngeo231.

Smedes, H. W. 1962. Lowland Creek Volcanics, an upper Oligocene formation near Butte, Montana. J. Geol. 70: 255–266.

Smedes, H.W., and Prostka, H.J., 1972, Stratigraphic Framework of the Absaroka Volcanic Supergroup in the Yellowstone National Park Region: U. S. Geological Survey Professional Paper 729-C, p. 1–43.

Sun, S.S., and McDonough, W.F., Chemical and isotopic systematics of oceanic basalts: implications for mantle composition and processes: Geological Society of London, Special Publications, v.42 (1), pp. 313-345, doi: 10/1144/GSL.SP.1989.042.01.19.

Sundell, K.A., 1993, A geologic overview of the Absaroka volcanic province. In: Snoke, A.W., Steidmann, J.R., Roberts, S.M. (Eds.), Geology of Wyoming. Geological Survey of Wyoming Memoir, vol. 5, pp. 480–506.

Syracuse, E.M., and Abers, G.A., 2006, Global compilation of variation in slab depth beneath arc volcanoes and implications: Arc volcano slab depth: Geochemistry, Geophysics, Geosystems, v. 7 (5), https://doi.org/10.1029/2005GC001045.

Taylor, R.D., Hammarstrom, J.M., Piatak, N.M., and Seal, Robert R., I., 2010, Arc-Related Porphyry Molybdenum Deposit Model: U.S. Geological Survey, Mineral Deposit Model for Resource Assessment, p. 1-64.

Tepper, J.H., and Clark, K.P., 2024, Initiation of the Cascade arc: Geology, v. XX, p. 1–5, doi:10.1130/g51888.1.

Tepper, J.M., Loewen, M.W., Caulfield, L.M., Davidson, P.C., Ruthenberg, K.L., Blakely, S.W.F., Knudsen, D.F.J.F., Black, D.F., Nelson, B.K., Asmerom, Y., 2023, Petrology and geochronology of Cretaceous – Eocene plutonic rocks in northeastern Washington, USA: Crustal thickening, slab rollback, and origin of the Challis episode: Geological Society of America Bulletin, p. 725 – 740, doi:10.1130/B36791.1.

Thoresen, H.E., Cassel, E.J., Smith, M.E., Stockli, D.F., and Jicha, B.R., 2024, Stratigraphic and geochronologic investigation of the Muddy Creek Basin: Implications for the Eocene tectonic evolution of southwest Montana, USA: Geological Society of America Bulletin, p. 1–15, doi:10.1130/b37268.1.

Tikoff, B., Housen, B.A., Maxson, J.., Nelson, E.M., Trevino, S., and Shipley, T.F., 2023, Hit-and-run model for Cretaceous–Paleogene tectonism along the western margin of Laurentia, *in* Laurentia: Turning Points in the Evolution of a Continent, Geological Society of America, v. 1220, p. 659–705, doi:10.1130/2022.1220(32).

U.S. Geological Survey, 2013, USGS 1/3 arc-second n44w113, n44w114, n45w113, n45w114, n45w115, n46w113, n47w113 1 x 1 degree: U.S. Geological Survey. https://apps.nationalmap.gov/downloader/#/

U.S. Geological Survey, 2019, USGS 1/3 arc-second n44w115, n44w116, n47w116 1 x 1 degree: U.S. Geological Survey. https://apps.nationalmap.gov/downloader/#/

U.S. Geological Survey, National Geospatial Technical Operations Center, 2020, USGS National Landcover - Woodland in Idaho State or Territory FileGDB 10.1: U.S. Geological Survey. https://apps.nationalmap.gov/downloader/#/

U.S. Geological Survey, National Geospatial Technical Operations Center, 2020, USGS National Landcover - Woodland in Montana State or Territory FileGDB 10.1: U.S. Geological Survey. https://apps.nationalmap.gov/downloader/#/

U.S. Geological Survey, National Geospatial Technical Operations Center, 2020, USGS National Landcover - Woodland in Wyoming State or Territory FileGDB 10.1: U.S. Geological Survey. https://apps.nationalmap.gov/downloader/#/

U.S. Geological Survey, 2022, USGS 1/3 arc-second n45w116, n46w116 1 x 1 degree: U.S. Geological Survey. https://apps.nationalmap.gov/downloader/#/

U.S. Geological Survey, 2023, USGS 1/3 arc-second n46w114, n46w115, n47w114, n47w115 1 x 1 degree: U.S. Geological Survey. https://apps.nationalmap.gov/downloader/#/

Van Hunen, J., Van Den Berg, A.P., and Vlaar, N.J., 2002, On the role of subduction oceanic plateaus in the development of shallow flat subduction: Tectonophysics, v. 352 (3-4), p. 317-333.

Van Kekan, P.E., Hacker, B.R., Syracuse, E.M., and Abers, G.A., 2011, Subduction factory: Depth-dependent flux of H2O from subducting slabs worldwide: Journal of Gephysical Research: Solid Earth, v. 116 (B1).

Vuke, S.M., Porter, K.W., Lonn, J.D., and Lopez, D.A., 2007, Geologic Map of Montana, Montana Bureau of Mines and Geology, https://gis-data-hub-mbmg.hub.arcgis.com/apps/53bf38cf17fd45dbbcf93b6cafaa3365/explore.

Weeks, C., 2022, Post-Laramide Exhumation and Topography in the Madison and Gallatin Ranges of Southwest Montana From Apatite (U-Th)/He Thermochronometry:, doi:10.1130/abs/2022am-383261.

Weil, A.B., and Yonkee, W.A., 2012, Layer-parallel shortening across the Sevier fold-thrust belt and Laramide foreland of Wyoming: Spatial and temporal evolution of a complex geodynamic system: Earth and Planetary Science Letters, v. 357–358, p. 405–420, doi:10.1016/j.epsl.2012.09.021.

Wells, M.L., Hoisch, T.D., Cruz-Uribe, A.M., and Vervoort, J.D., 2012, Geodynamics of synconvergent extension and tectonic mode switching: Constraints from the Sevier-Laramide orogen: Tectonics, v. 31, p. 1–20, doi:10.1029/2011TC002913.

Wells, R., Bukry, D., Friedman, R., Pyle, D., Duncan, R., Haeussler, P., and Wooden, J., 2014, Geologic history of Siletzia, a large igneous province in the Oregon and Washington Coast Range: Correlation to the geomagnetic polarity time scale and implications for a long-lived Yellowstone hotspot: Geosphere, v. 10, p. 692–719, doi:10.1130/GES01018.1.

Whitney, M.S., 1975, Geology of the CUMO Prospect [M.S. Thesis]: Colorado School of Mines, 97 p.

Wiemer, D., Hagemann, S.G., Hayward, N., Begg, G.C., Hronsky, J., Thébaud, N., Kemp, A.I.S., and Villanes, C., 2023, Cryptic trans-lithospheric fault systems at the western margin of South America: implications for the formation and localization of gold-rich deposit superclusters: Front. Earth Sci., v. 11, 1159430, doi:10.3389/feart.2023.1159430.

Worthington, J.E., 2007, Porphyry and other molybdenum deposits of Idaho and Montana: Idaho Geological Survey Technical Report 07-3, p. 18.

Wyoming State Geological Survey. "Wyoming Bedrock Geology." *Wyoming State Geological Survey*, 2013, www.wsgs.wyo.gov/pubs-maps/gis.aspx.

Young-Dahl, E.E., 2021, Reconstructing Eocene Paleotopography of the Northern U.S. Cordillera Using Stable Isotope Paleoaltimetry of Hydrated Volcanic Glass: University of Idaho , 82 p.

Yonkee, W.A., and Weil, A.B., 2015, Tectonic evolution of the Sevier and Laramide belts within the North American Cordillera orogenic system: Earth-Science Reviews, v. 150, p. 531–593, doi:10.1016/j.earscirev.2015.08.001.

Appendix A - GIS Data

Appendix Figure A.1 – State boundary polygon shapefiles for the State of Idaho, State of Montana, and State of Wyoming using the NAD 1983 (2011) geographic coordinate system.

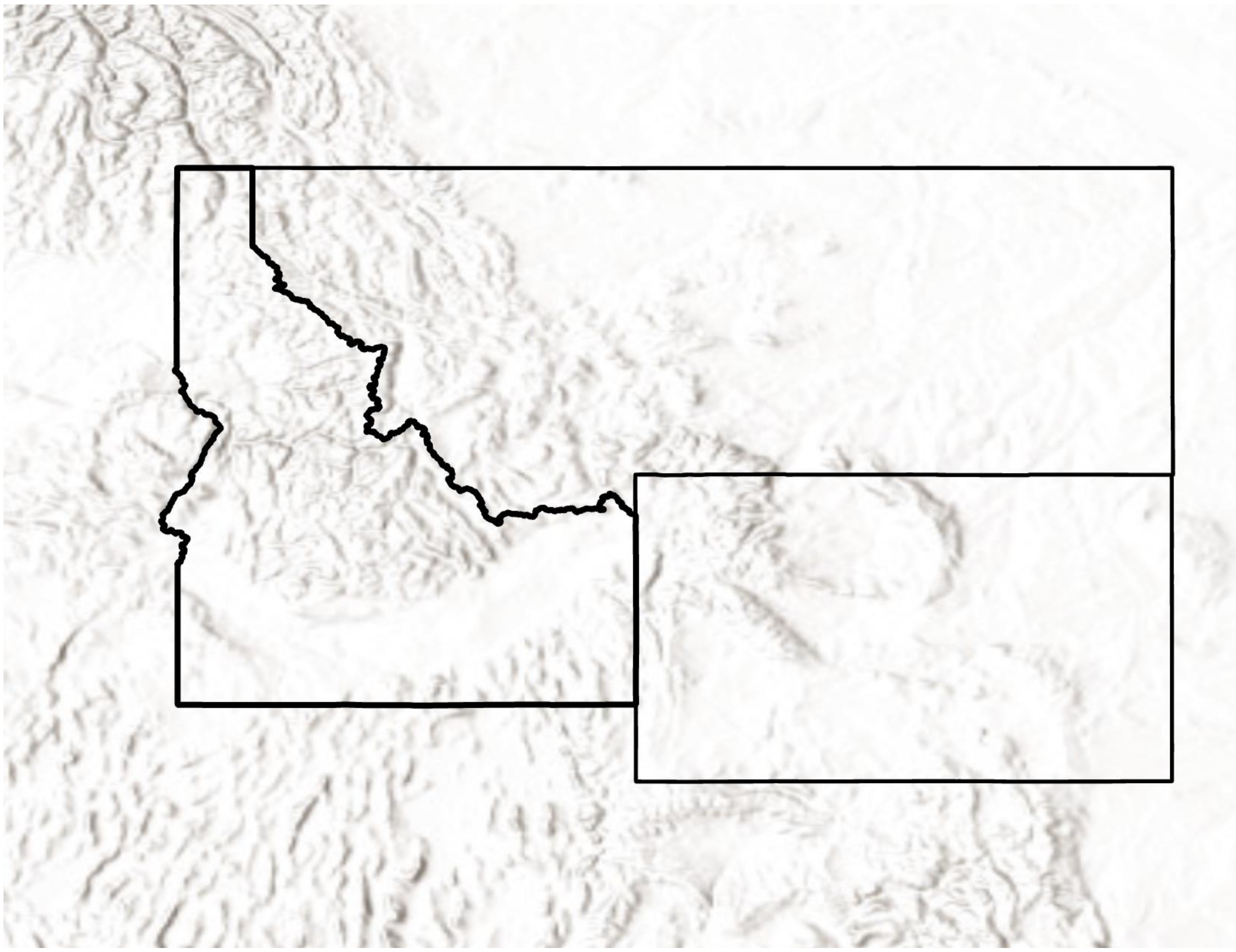

Appendix Figure A.2 – Geologic units polygon shapefiles for the State of Idaho, State of Montana, and State of Wyoming with symbology set to unique values and using unit name values. The geographic coordinate system is set to NAD 1983 (2011).

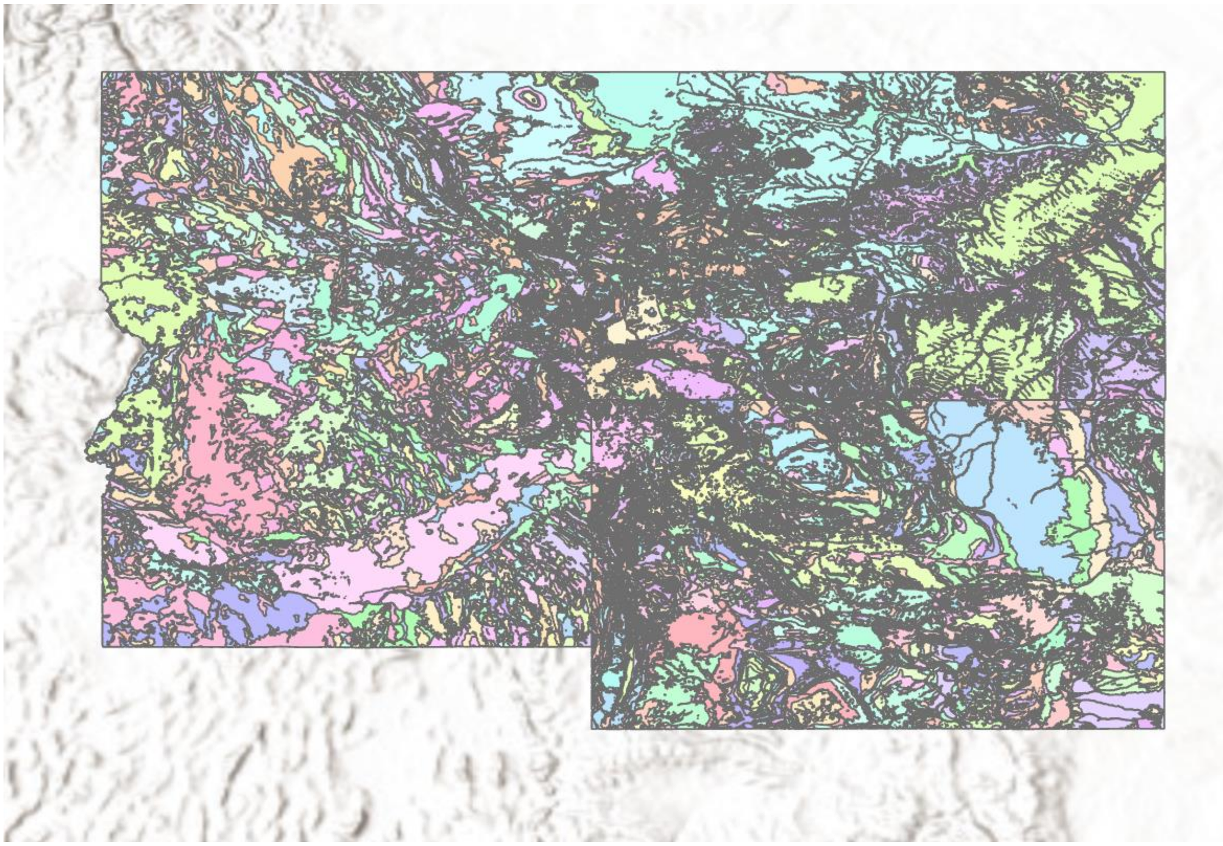

Appendix Figure A.3 – Geologic polyline files set to the NAD 1983 (2011) geographic coordinate system for the State of Idaho, State of Montana, and State of Wyoming.

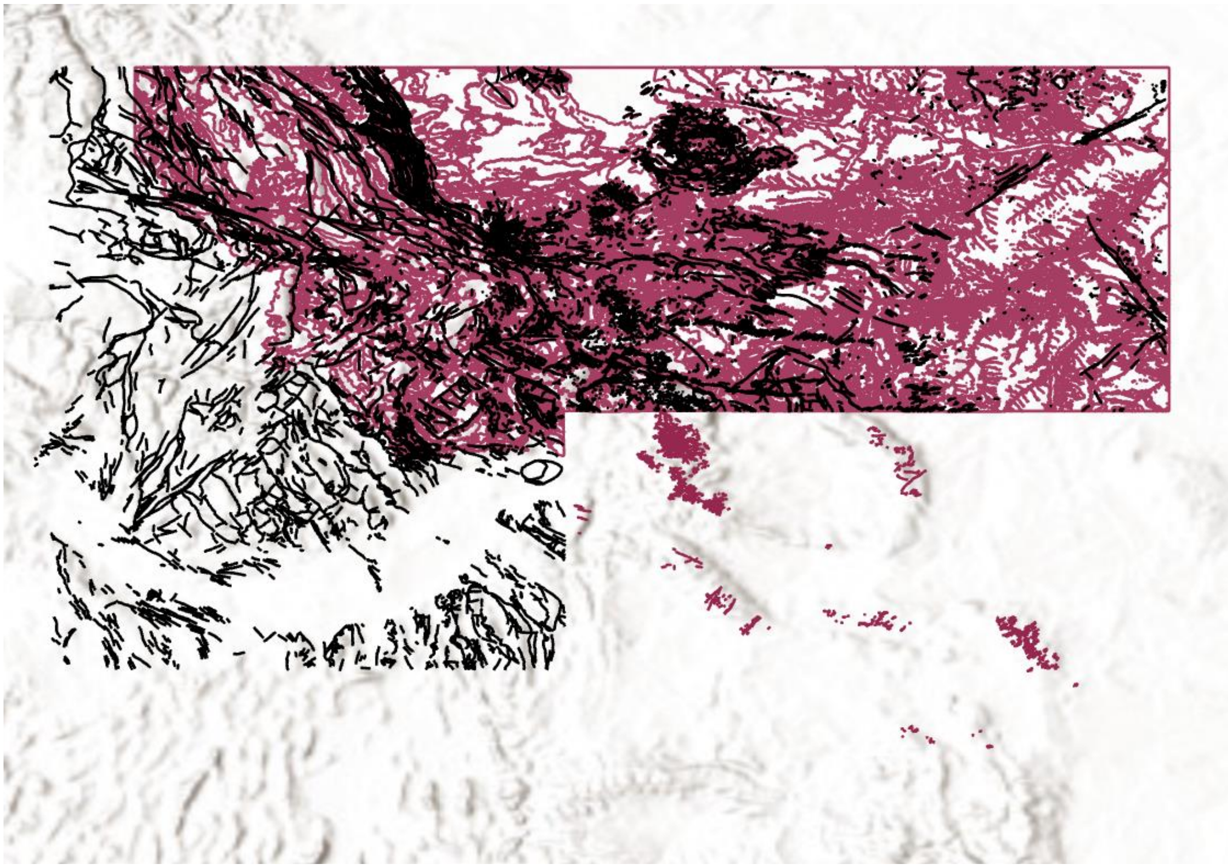

Appendix Figure A.4 – Yellowstone National Park boundary shapefile using the NAD 1983 (2011) geographic coordinate system.

Appendix Figure A.5 – National elevation 1 arc-second raster datasets: 46.001667 degrees to 42.998333 degrees and -112.001667 degrees to -107.998333 degrees (Absaroka volcanic region); 47.000556 degrees to 42.999444 degrees and -116.000556 degrees to -112.999444 degrees (central Idaho Challis volcanic region); 47.000556 degrees to 44.999444 degrees and -114.000556 degrees to -111.999444 degrees (Lowland Creek volcanic region).

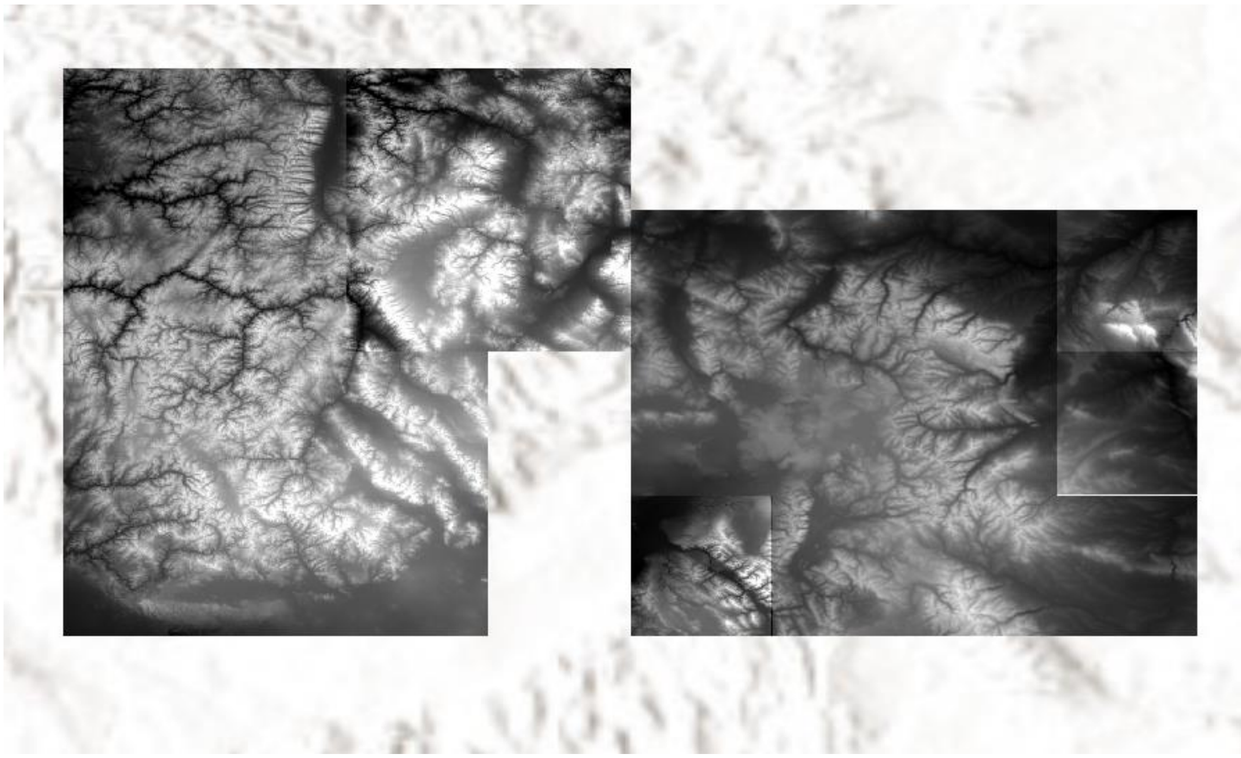

Appendix B - Bulk Rock Geochemistry

Bulk rock geochemical data associated with this study can be found in the attached supplementary Excel file titled: KyleBroley2024GeochemicalData

- Bulk rock geochemical data for the Absaroka volcanic province is from:

Feeley, T.C., Cosca, M.A., and Lindsay, C.R., 2002, Petrogenesis and implications of calc-alkaline cryptic hybrid magmas from Washburn volcano, Absaroka Volcanic Province, USA: Journal of Petrology, v. 43, p. 663–703, doi:10.1093/petrology/43.4.663.

Hiza, M.M., 1999, The geochemistry and geochronology of the Eocene Absaroka volcanic province, northern Wyoming and southwest Montana, USA [Ph.D. Thesis]: Oregon State University, 243 p.

Lindsay, C.R., and Feeley, T.C., 2003, Magmagenesis at the Eocene Electric Peak-Sepulcher Mountain complex, Absaroka Volcanic Province, USA: Lithos, v. 67, p. 53–76, doi:10.1016/S0024-4937(02)00252-9.

- Bulk rock geochemical data for the central Idaho Challis volcanic province is from:

Gaschnig, R.M., Vervoort, J.D., Lewis, R.S., and Tikoff, B., 2011, Isotopic evolution of the Idaho batholith and Challis intrusive province, Northern US Cordillera: Journal of Petrology, v. 52, p. 2397–2429, doi:10.1093/petrology/egr050.

McKervey, John Antony, 1998, The petrogenesis of the Eocene Challis Volcanic Group, Idaho, western U.S.A. [Ph.D. thesis]: The Open University, 365 p.

Norman, M.D., and Mertzman, S.A., 1991, Petrogenesis of Challis volcanics from central and southwestern Idaho: trace element and Pb isotopic evidence: Journal of Geophysical Research, v. 96, p. 13,279-13,293, doi:10.1029/91jb00285.

- Bulk rock geochemical data for the Lowland Creek volcanic province is from:

Dudás, F.Ö., Ispolatov, V.O., Harlan, S.S., and Snee, L.W., 2010, 40Ar/39Ar geochronology and geochemical reconnaissance of the Eocene Lowland Creek volcanic field, west-central Montana: Journal of Geology, v. 118, p. 295–304, doi:10.1086/651523.

Scarberry, K.C., Yakovlev, P. V, and Schwartz, T.M., 2011, Mesozoic Magmatism in Montana: MBMG Special Publication 122: Geology of Montana, v. 1, p. 30.